Cycle of GAS and STARS in Galaxies

- *Gas is transformed into stars*
- *Each star burns H and He in its nucleus and produces heavy elements*
- *These elements are partially returned into the interstellar gas at the end of the star's life*
  - *Through winds and supernovae explosions*
  - *Some fraction of the metals are locked into the remnant of the star*

This implies that the chemical abundance of the gas in a star-forming galaxy should evolve with time

Life-cycle of low mass stars like the sun

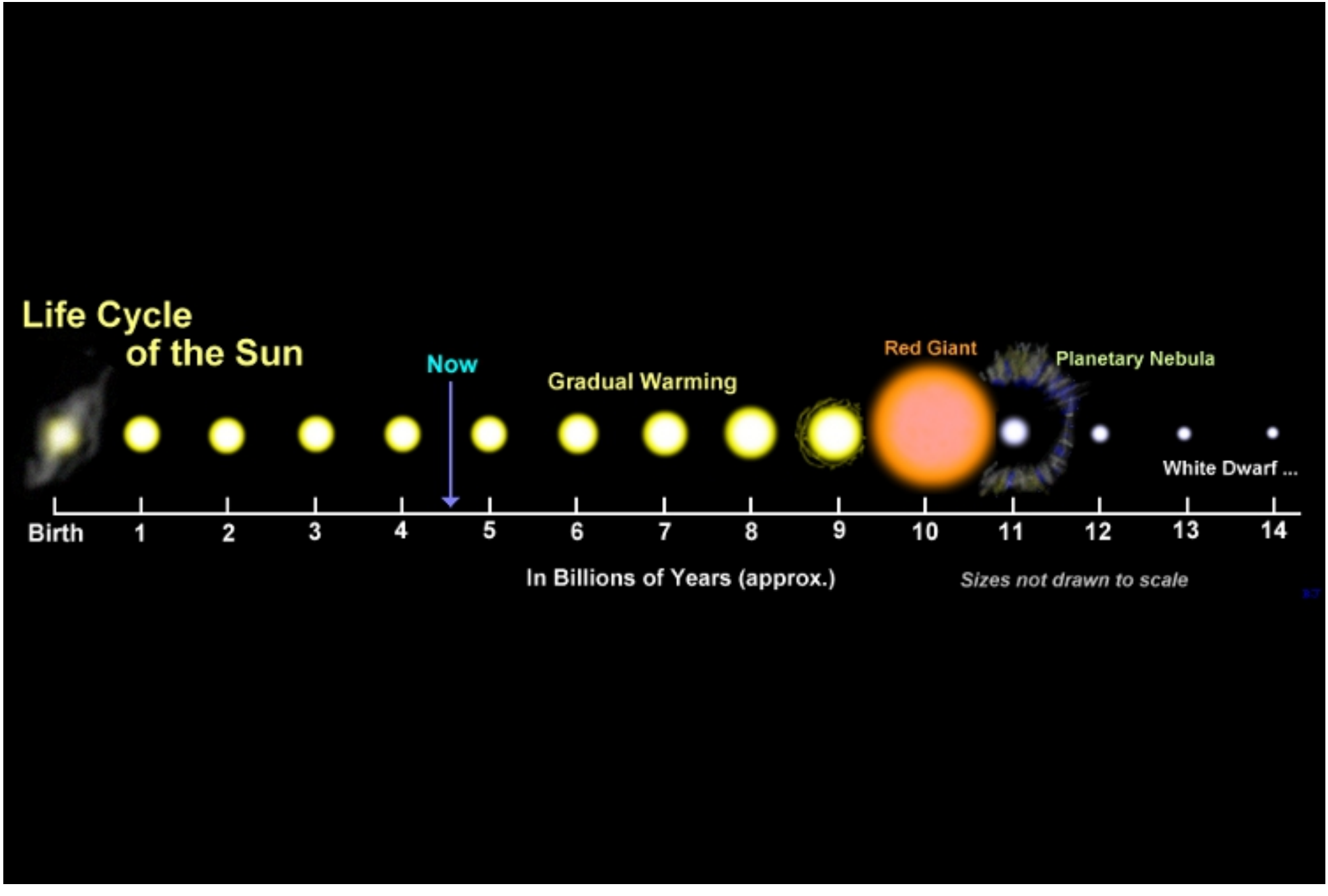

Mass ejection from stars like our sun (Planetary Nebulae)

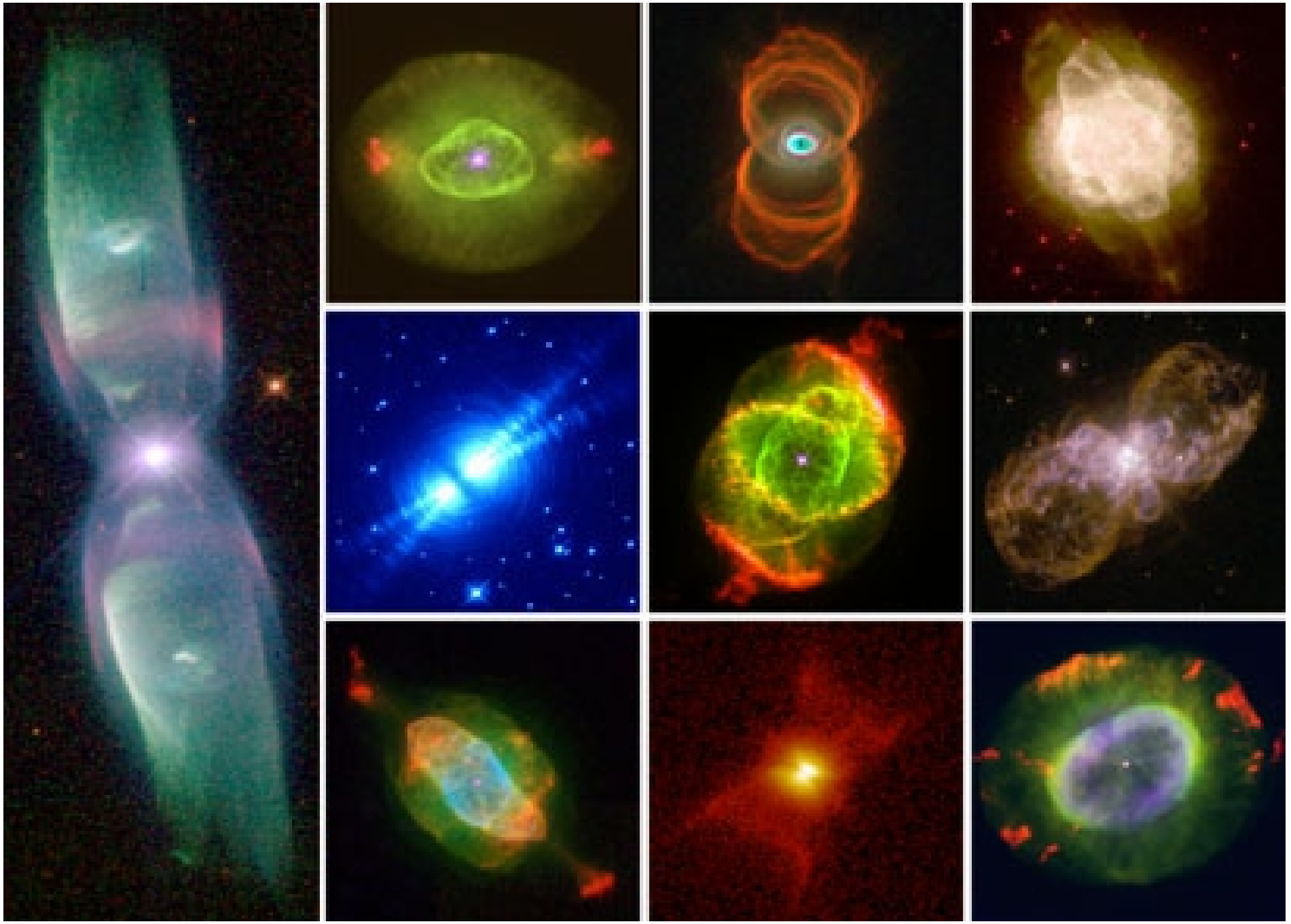

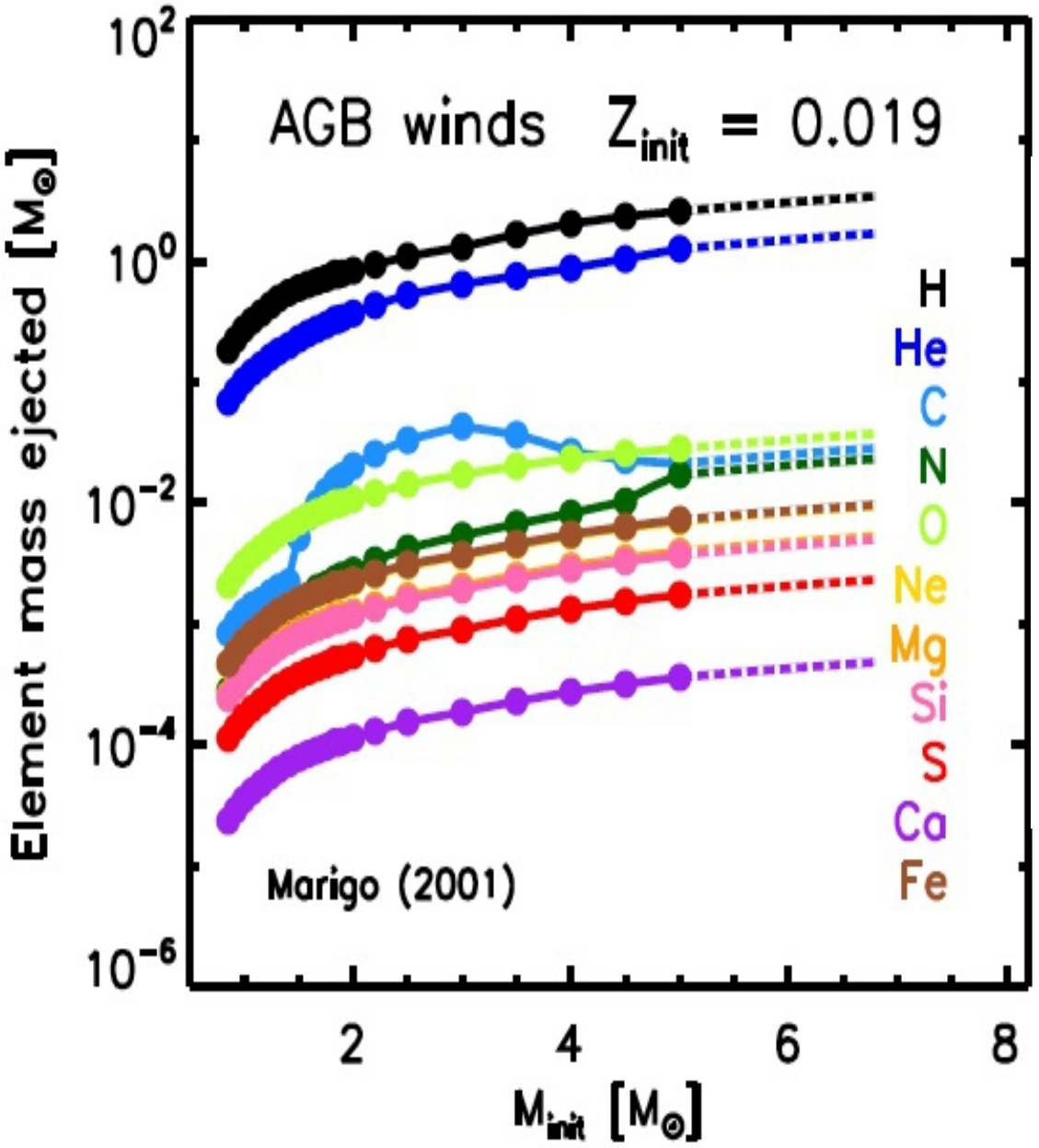

Chemical composition of the Sun

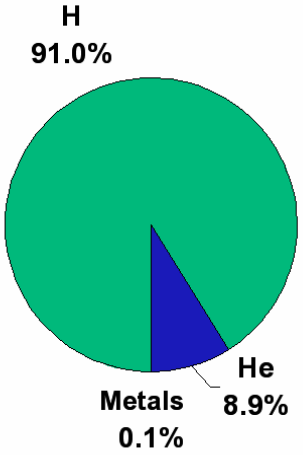

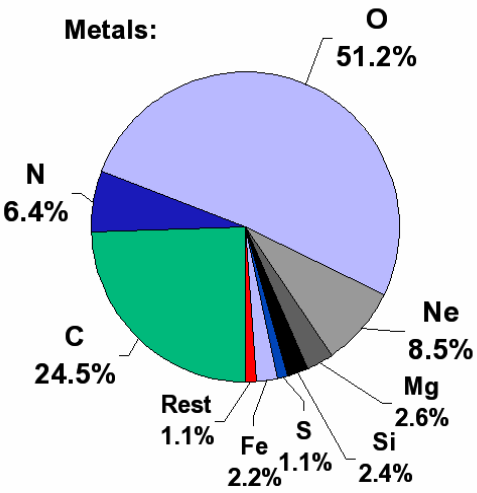

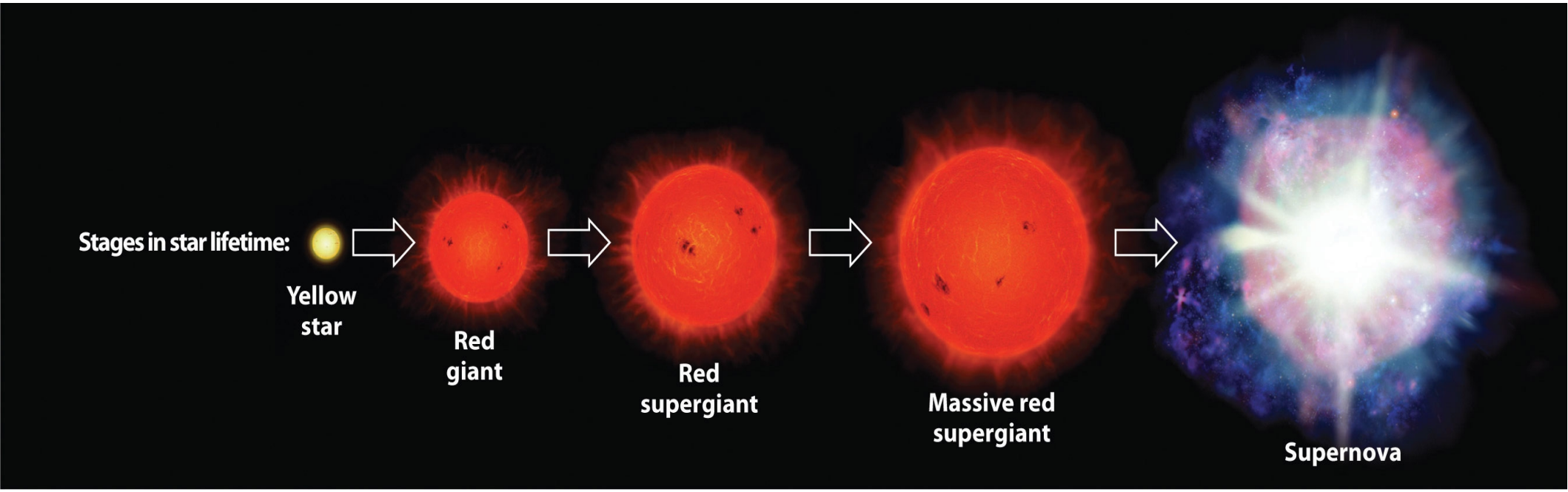

Core Temperature:	1.5×10^7 K	2×10^8 K	7×10^8 K	3×10^9 K	1×10^{11} K
Primary Nuclear Reaction:	^{1}H fusion	^{4}He fusion	$^4\text{He} + {}^{12}\text{C}$ $^{12}\text{C} + {}^{12}\text{C}$ $^{12}\text{C} + {}^{16}\text{O}$	Proton–neutron exchange reactions	Multiple neutron captures
Elements Formed:	He	C, O, Ne, Mg	Na, Si, S, Ar, Ca	Fe, Ni	Elements with $Z > 28$

Stars more mass than 8 M (sun) end their lives in supernova explosions

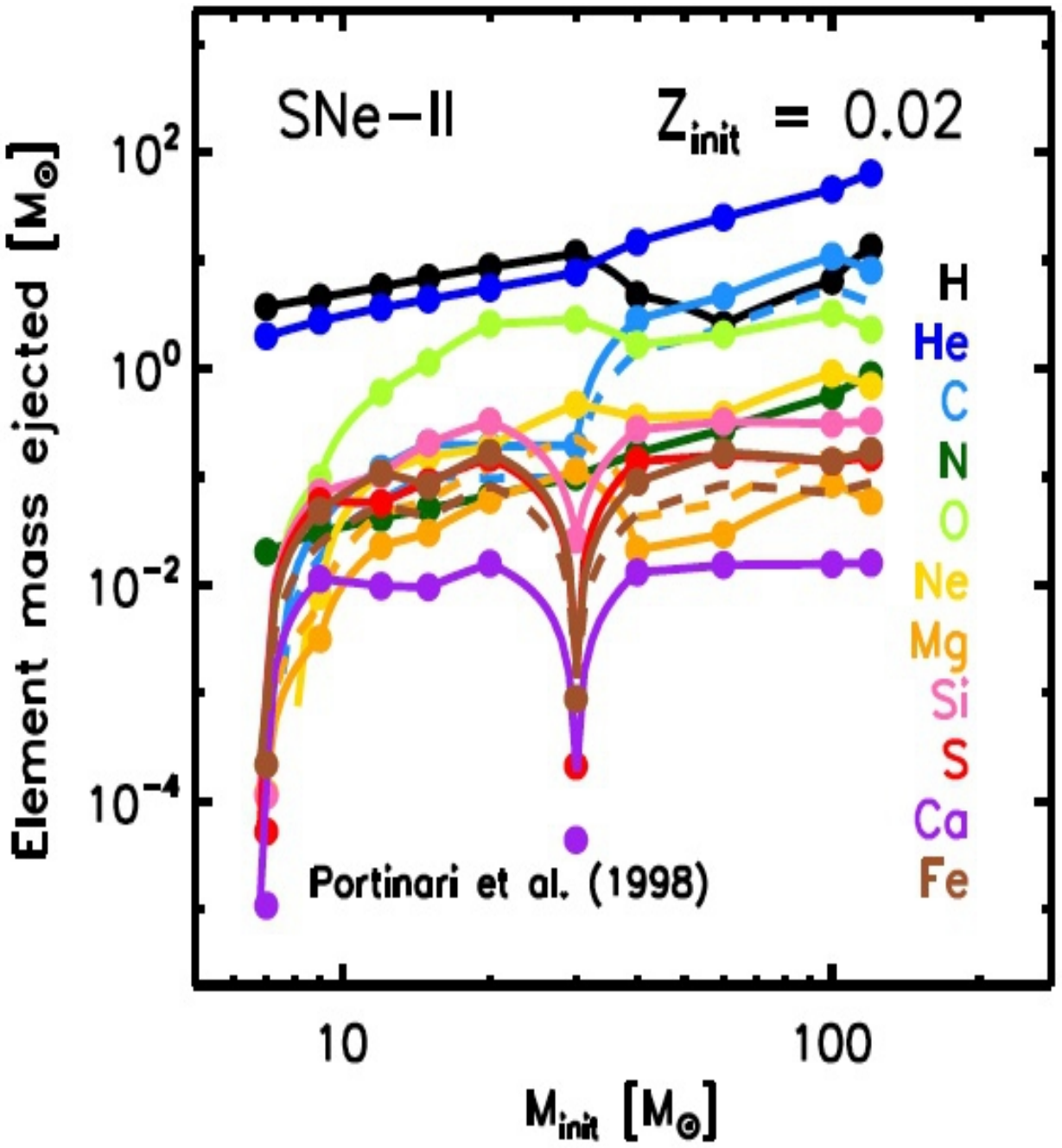
SNe−II
Z_{init} = 0.02
10^2
10^0
10^{-2}
10^{-4}
Element mass ejected [$M_\odot$]
H
He
C
N
O
Ne
Mg
Si
S
Ca
Fe
Portinari et al. (1998)
10
100
M_{init} [$M_\odot$]

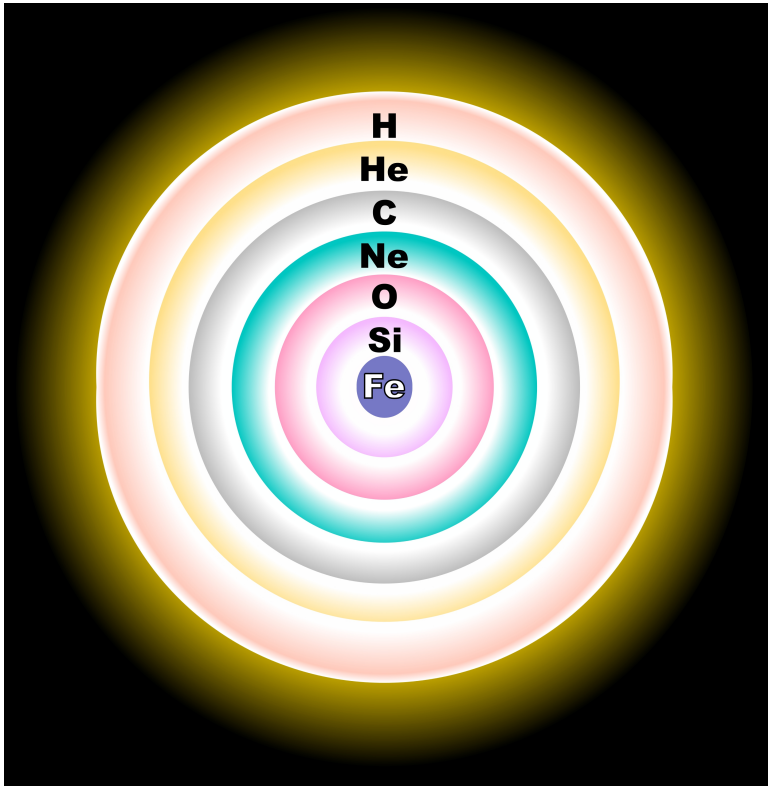
H
He
C
Ne
O
Si
Fe

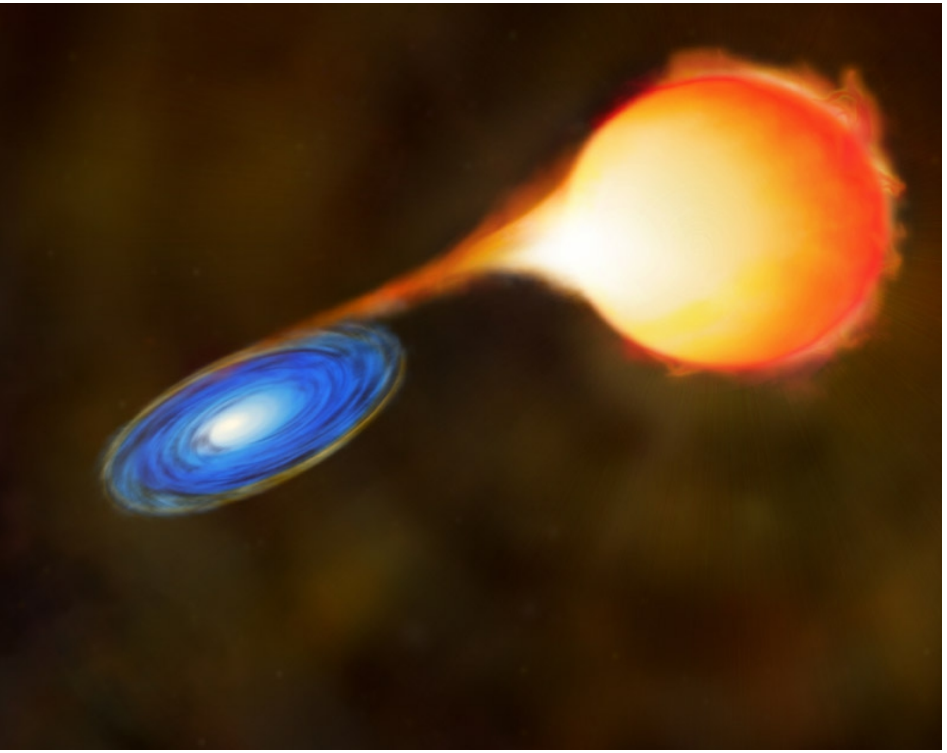

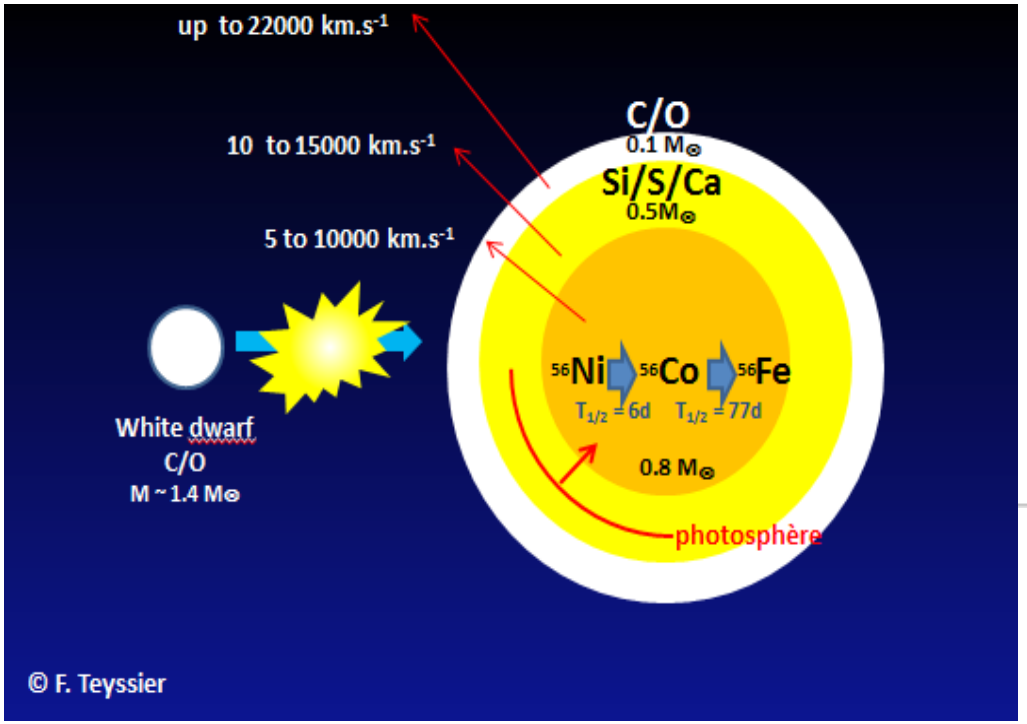
up to 22000 km.s-1
10 to 15000 km.s-1
5 to 10000 km.s-1
C/O
0.1 M⊙
Si/S/Ca
0.5M⊙
56Ni
56Co
56Fe
T1/2 = 6d
T1/2 = 77d
0.8 M⊙
photosphère
White dwarf
C/O
M ~ 1.4 M⊙
© F. Teyssier

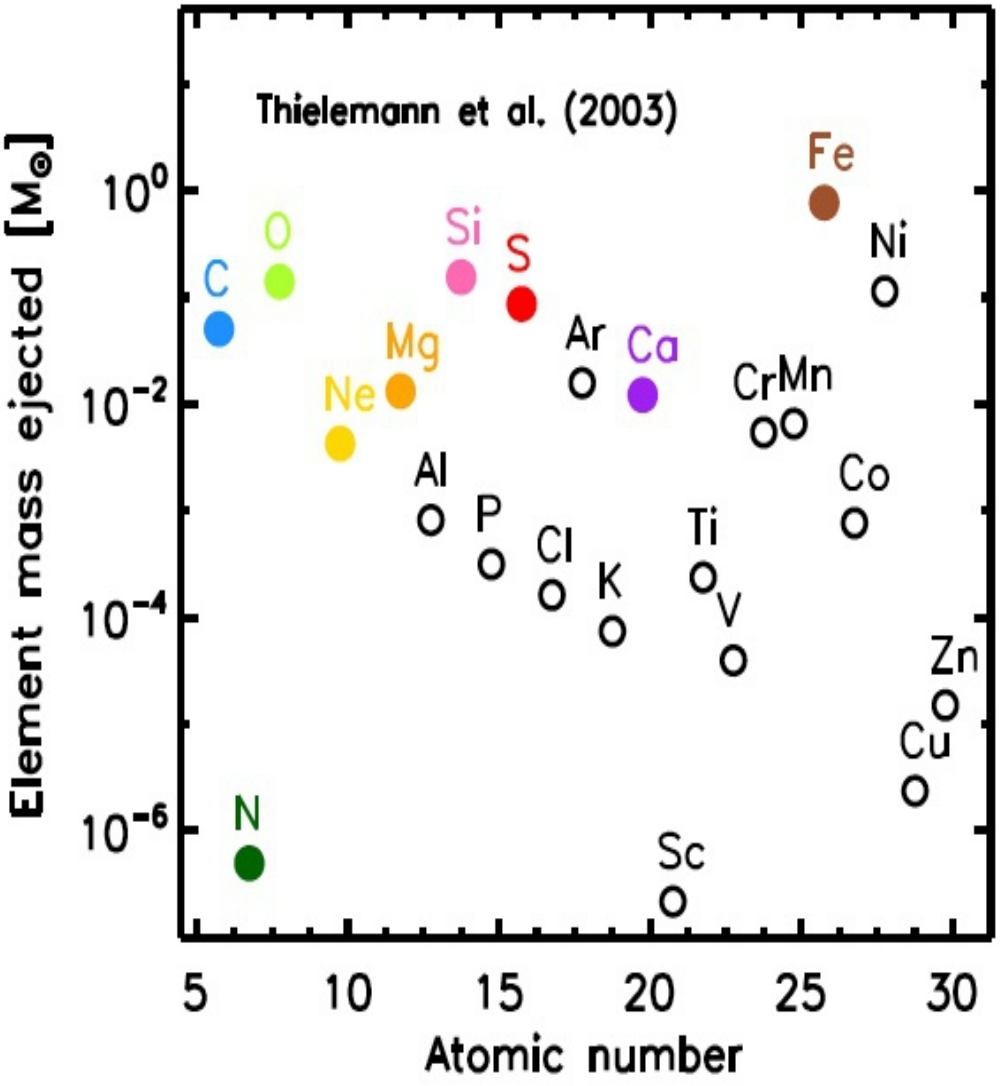
Thielemann et al. (2003)
Element mass ejected [M⊙]
Atomic number
10^0
10^-2
10^-4
10^-6
5
10
15
20
25
30
C
O
Si
S
Fe
Ni
Ne
Mg
Ar
Ca
Cr
Mn
Co
Al
P
Cl
K
Ti
V
Zn
Cu
N
Sc

Modeling Chemical Evolution

To start, let's consider the types of parameters and variables that are involved. First, there are the global variables, all of which are a function of time.

M_g: Total mass of interstellar gas
M_s: Total mass of stars
M_w: Total mass of stellar remnants (white dwarfs)
M_t: Total mass of the system
E: the rate of mass ejection from stars
E_Z: the rate of metal ejection from stars
W: the creation rate of stellar remnants.

Naturally, $M_t = M_g + M_s + M_w$.

Ψ: Rate of star formation
f: Rate of infall or outflow of material from the system
Z_f: Metal abundance of the infall (or outflow) material
$\phi(m)$: the Initial Mass Function

w: the mass of a stellar remnant

τ_m: the main-sequence lifetime of a star

m_{tn}: the turnoff mass of a population with $t = \tau$

p_z: the stellar recyclable mass fraction that is converted to metal z and then ejected into space.

Given the above variables and parameters, the goal is to derive $Z(t)$, the fraction of metals (individually, or as a group) in the interstellar medium as a function of time.

Equations of Chemical Evolution

$$\frac{dM_t}{dt} = f$$

Total mass conservation

$$\frac{dM_s}{dt} = \Psi - E - W$$

Change in stellar mass

$$\frac{dM_g}{dt} = -\Psi + E + f$$

Change in gas mass

$$\frac{dM_w}{dt} = W$$

Change in remnant mass

$$\frac{d(ZM_g)}{dt} = -Z\Psi + E_Z + Z_f f$$

Change in metals:

1) metals locked up in stars
2) metals released by stars
3) metals added from/lost to the external medium

Relate mass return , stellar remnant formation, and metal input rates to stellar parameters

$$E = \int_{m_{tn}}^{m_u} (m - w)\Psi(t - \tau_m)\phi(m, t - \tau_m)dm$$

where m_u is the upper mass limit of the stellar IMF, and m_{tn}, the turnoff mass at time t. Similarly, the equation for the total mass of remnants formed is

$$W = \int_{m_{tn}}^{m_u} w\Psi(t - \tau_m)\,\phi(m, t - \tau_m)dm$$

The equation for E_Z is a bit more complicated since it has two terms: one to represent the amount of *new* metals created by a star and released during mass loss, and a second to represent the amount of metals that were lost from the ISM when the star formed, but are now being re-released. Mathematically, this is

$$E_Z = \int_{m_{tn}}^{m_u} mp_z\Psi(t - \tau_m)\,\phi(m, t - \tau_m)dm +$$
$$\int_{m_{tn}}^{m_u} (m - w - mp_z)Z(t - \tau_m)\Psi(t - \tau_m)\,\phi(m, t - \tau_m)dm$$

Finally, there is an equation of metal conservation. If $\bar{Z}_s$ is the average metal content in stars, then the total amount of metals produced in a galaxy over a Hubble time is

$$\bar{Z}_s M_s + Z M_g = \int_0^t \int_{m_{tn}}^{m_u} m p_z \Psi(t' - \tau_m) \phi(m, t' - \tau_m) dt' dm$$

SIMPLIFICATIONS

1) The initial mass function of stars is independent of time. That is, φ(m,t) = φ(m).

2) Instantaneous recycling approximation. The approximation says that there are two types of stars in a galaxy: those that live forever, and those that evolve and die instantaneously.

Main Sequence Lifetimes

Spectral Type	Mass $(\mathcal{M}/\mathcal{M}_\odot)$	Luminosity $(\mathcal{L}/\mathcal{L}_\odot)$	Lifetime (years)
O5 V	60	7.9×10^5	5.5×10^5
B0 V	18	5.2×10^4	2.4×10^6
B5 V	6	820	5.2×10^7
A0 V	3	54	3.9×10^8
F0 V	1.5	6.5	1.8×10^9
G0 V	1.1	1.5	5.1×10^9
K0 V	0.8	0.42	1.4×10^{10}
M0 V	0.5	0.077	4.8×10^{10}
M5 V	0.2	0.011	1.4×10^{11}

Note the values. Stars with $\mathcal{M} > 5\mathcal{M}_\odot$ evolve in less than 10^8 years, which, in cosmological terms, is almost instantaneously. On the other hand, stars with mass less than about $1\mathcal{M}_\odot$ live forever. So the approximation only breaks down for a limited mass range.

Let's choose m_1 to be the dividing line between stars that live forever, and stars that evolve instantaneously. Let's also define three new quantities, the **Return fraction** of gas

$$R = \int_{m_1}^{\infty} (m - w)\phi(m)dm$$

the **Baryonic Dark Matter fraction**

$$D = \int_{m_1}^{\infty} w\phi(m)dm$$

and the **Net Yield** (of element i)

$$y_i = \frac{1}{1-R}\int_{m_1}^{\infty} mp_z\phi(m)dm$$

It can then be shown that $E = R^9\Psi$, $W = D\,\Psi$, and

$$E_Z = \Psi\{ZR + y_z(1-R)\}$$

With our two assumptions, the equations of chemical evolution become

$$\frac{d\mathcal{M}_t}{dt} = f$$

$$\frac{d\mathcal{M}_s}{dt} = (1 - R - D)\Psi$$

$$\frac{d\mathcal{M}_g}{dt} = -(1 - R)\Psi + f$$

$$\frac{d\mathcal{M}_w}{dt} = D\Psi$$

$$\frac{d(Z\mathcal{M}_g)}{dt} = -Z\Psi(1 - R) + y_z\Psi(1 - R) + Z_f f$$

Noting that:

$$\frac{d(Z\mathcal{M}_g)}{dt} = Z\frac{d\mathcal{M}_g}{dt} + \mathcal{M}_g\frac{dZ}{dt}$$

Substituting for dM_g/dt then yields

$$\mathcal{M}_g\frac{dZ}{dt} = y_z\Psi(1 - R) + (Z_f - Z)f$$

The Closed Box Model of Chemical Evolution

As an example of what a chemical evolution model can do, consider a closed system, where all the material for current star formation comes from mass lost by a previous generation of stars. In this case, there is no infall, and, from (9.23),

$$\mathcal{M}_g \frac{dZ}{dt} = y_z \Psi (1 - R) + (Z_f - Z) f = y_z \Psi (1 - R)$$

In addition,

$$\frac{d\mathcal{M}_g}{dt} = -(1 - R)\Psi + f = -(1 - R)\Psi$$

By dividing these two equations, we get

$$\mathcal{M}_g \frac{dZ}{dt} \Big/ \frac{d\mathcal{M}_g}{dt} = \mathcal{M}_g \frac{dZ}{d\mathcal{M}_g} = -y_z$$

Since y_z is a constant of stellar evolution

$$\int_{Z_0}^{Z_1} dZ = -y_z \int_{\mathcal{M}_{g0}}^{\mathcal{M}_{g1}} \frac{d\mathcal{M}_g}{\mathcal{M}_g} \Longrightarrow \boxed{Z_1 - Z_0 = -y_z \ln\left(\frac{\mathcal{M}_{g0}}{\mathcal{M}_{g1}}\right)}$$

where Z_0 and $\mathcal{M}_{g0}$ represent the initial metallicity and gas mass of the galaxy, and Z_1 and $\mathcal{M}_{g1}$ represent those quantities today.

Note that if we measure gas-phase metallicities and gas masses for galaxies, we can deduce the net yield y_Z. If the closed box model is correct, y_Z should be constant, i.e. A TEST

Prediction 2: Metallicity distribution of stars

Define $\mu=M_g/M_t$, $\sigma=M_s/M_t$ The closed-box solution gives:

$$\mu_1 = \mu_0 \exp\left\{-\frac{Z_1 - Z_0}{y_z}\right\}$$

In other words, as the system evolves, the gas fraction will decrease exponentially with Z.

Take the derivative with respect to Z:

$$\frac{d\mu}{dZ} = -\frac{\mu_1}{y_z} \exp\left\{-\frac{Z_1 - Z_0}{y_z}\right\}$$

$$\frac{d\mathcal{M}_s}{dt} \Big/ \frac{d\mathcal{M}_g}{dt} = \frac{d\sigma}{d\mu} = -\frac{(1-R-D)}{(1-R)}$$

so

$$\frac{d\sigma}{dZ} = \left(\frac{d\mu}{dZ}\right)\left(\frac{d\sigma}{d\mu}\right) = \left(\frac{\mu}{y_z}\right)\left(\frac{1-R-D}{1-R}\right)\exp\left\{-\frac{Z_1-Z_0}{y_z}\right\}$$

Finally, if we put this equation in terms of $\log Z$, instead of Z, then

$$\frac{d\sigma/\sigma_1}{d\log Z} = (\ln 10)\left(\frac{Z_0}{y_z}\right)\left(\frac{1-R-D}{1-R}\right)\left(\frac{\mu_1}{\sigma_1}\right)\exp\left\{-\frac{Z_1-Z_0}{y_z}\right\}$$

Predicted metallicity distribution of stars

Measurement of gas-phase metallicities through nebular emission lines

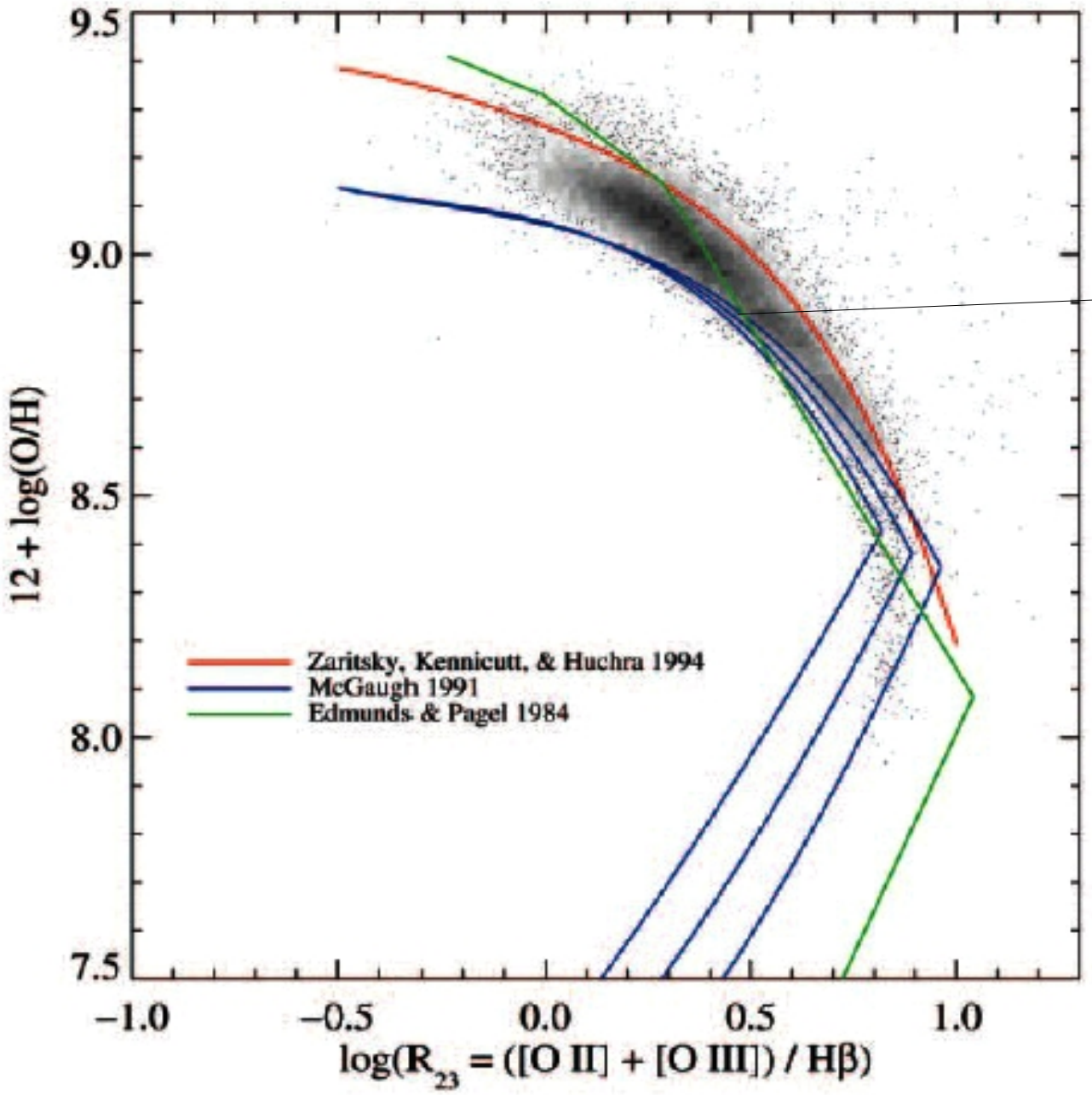

Calibration of metallicity using photo-ionization models

RELATION BETWEEN GAS-PHASE METALLICITY AND STELLAR MASS

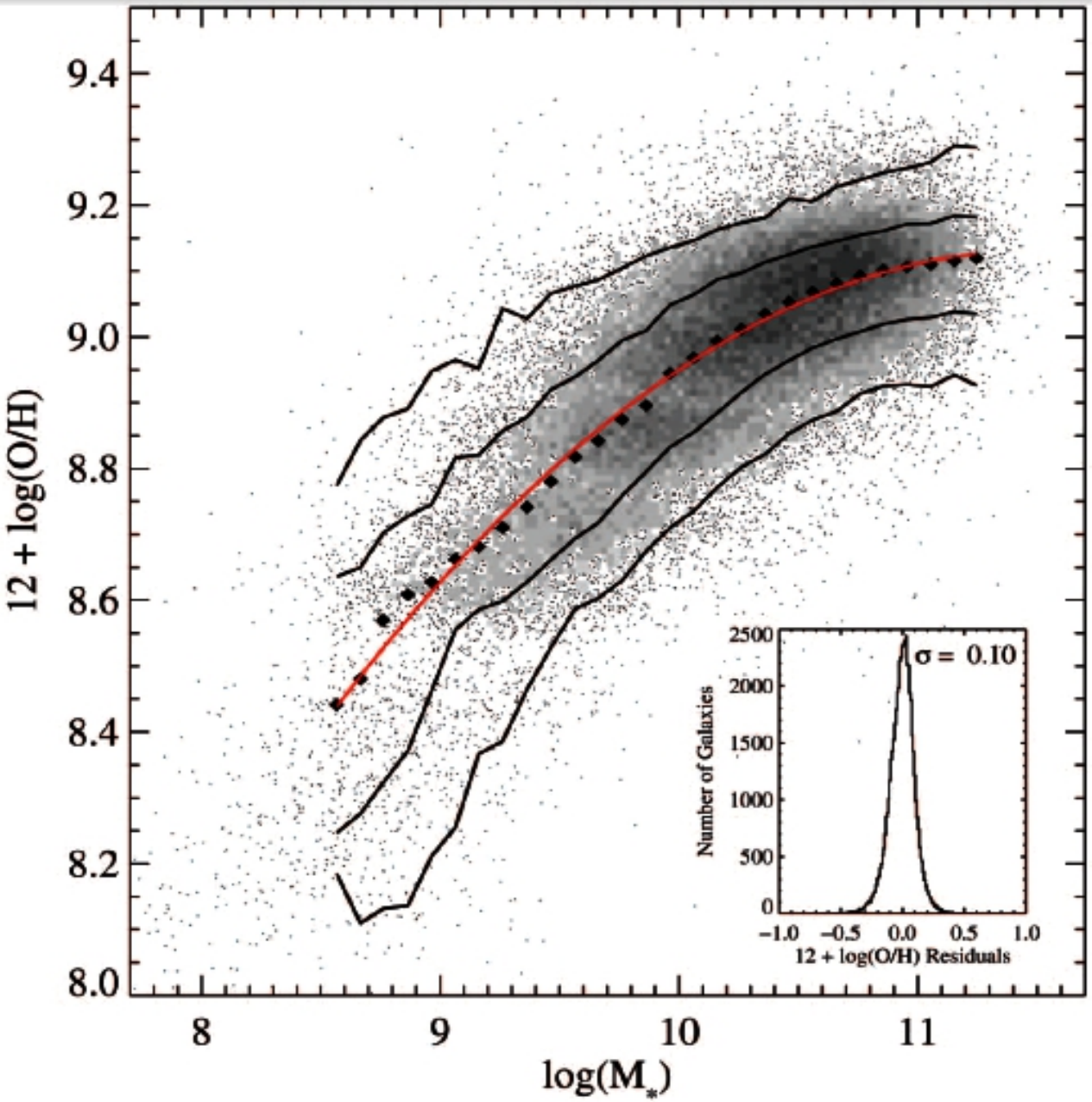

The net yield decreases in low mass galaxies, indicating

LOSS OF METALS

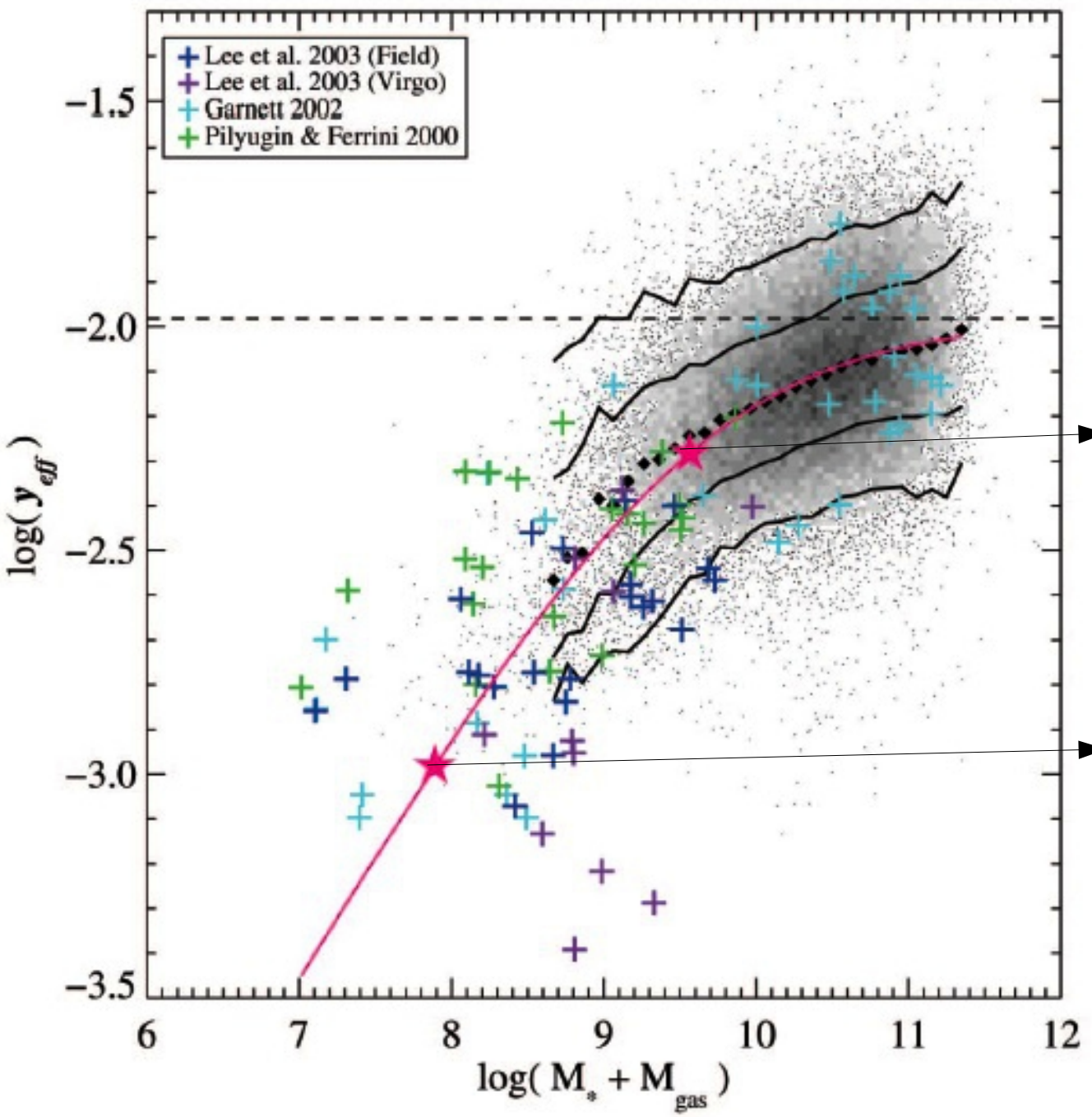

Metallicity distribution of bulge stars follows prediction of closed-box model

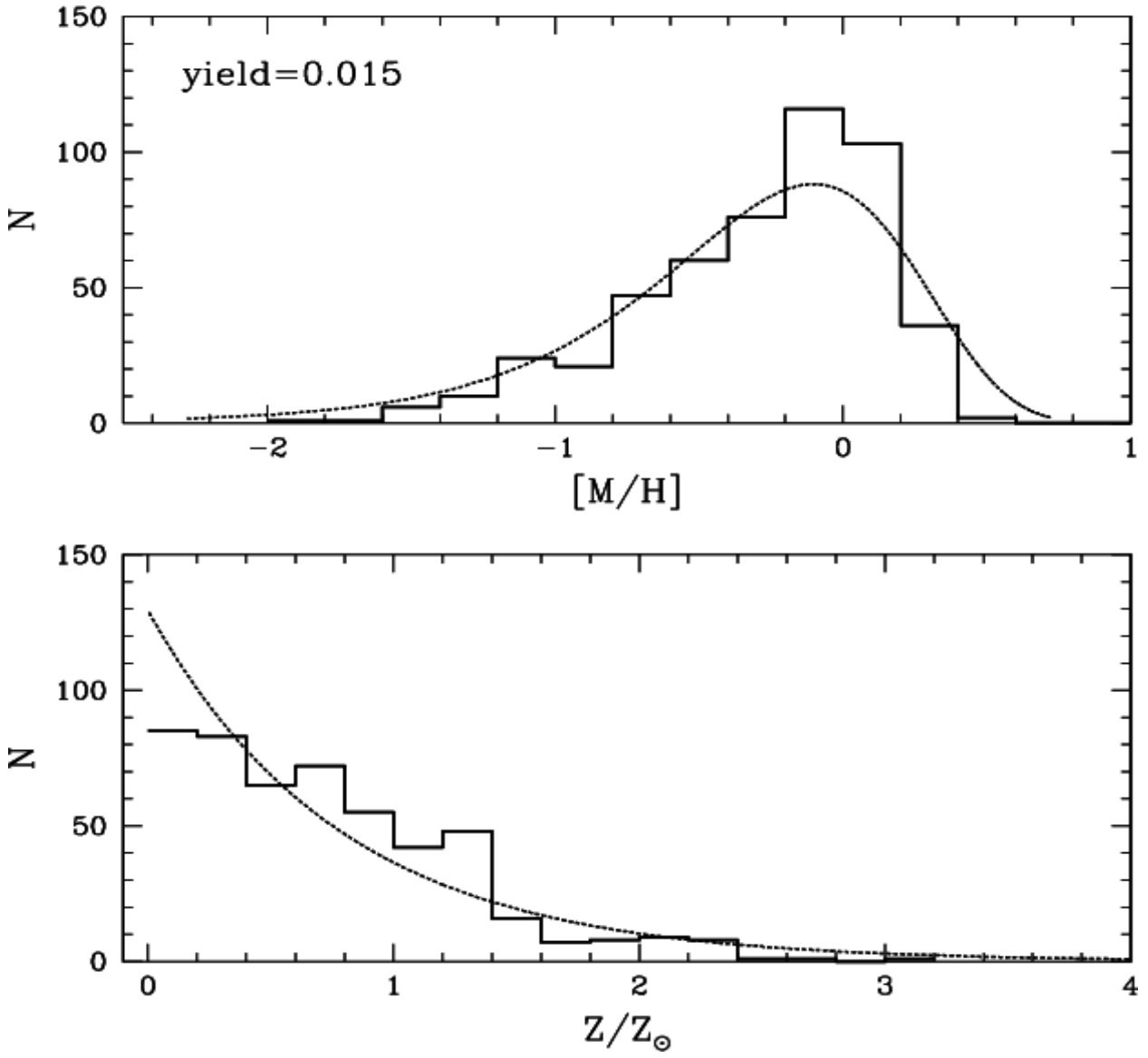

The metallicity distribution of disk stars does not....

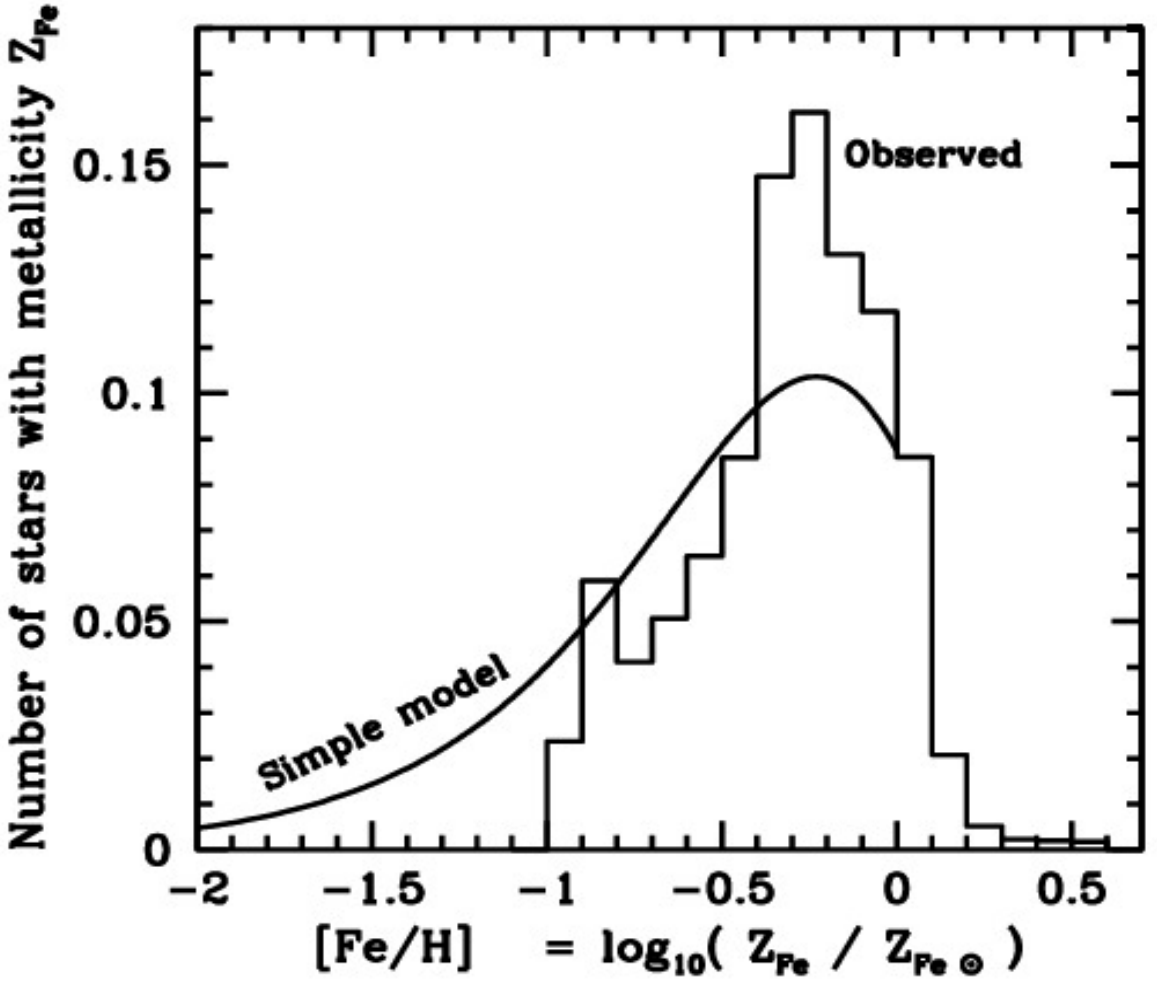

The observed differential metallicity distribution for stars in the solar neighbourhood, compared with the Simple Model prediction for $p = 0.010$ and $Z_1 = Z_\odot = 0.017$. [The observed distribution uses data from Kotoneva et al., M.N.R.A.S., 336, 879, 2002, for stars in the Hipparcos Catalogue.]

Expulsion of gas and metals from galaxies occurs as a result of a **galactic wind** powered by many supernovae explosions

The Starburst Dwarf Galaxy NGC 3079

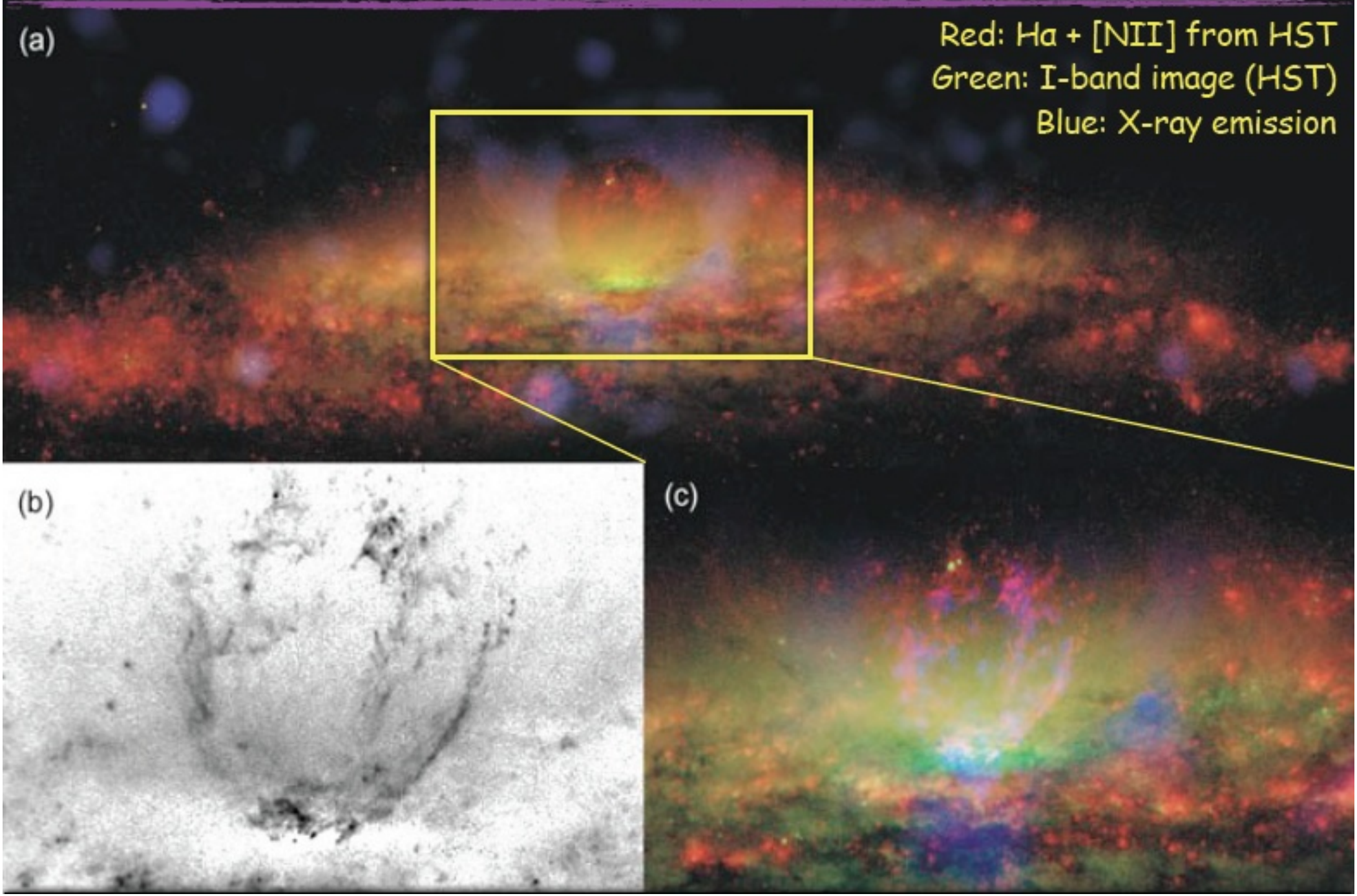

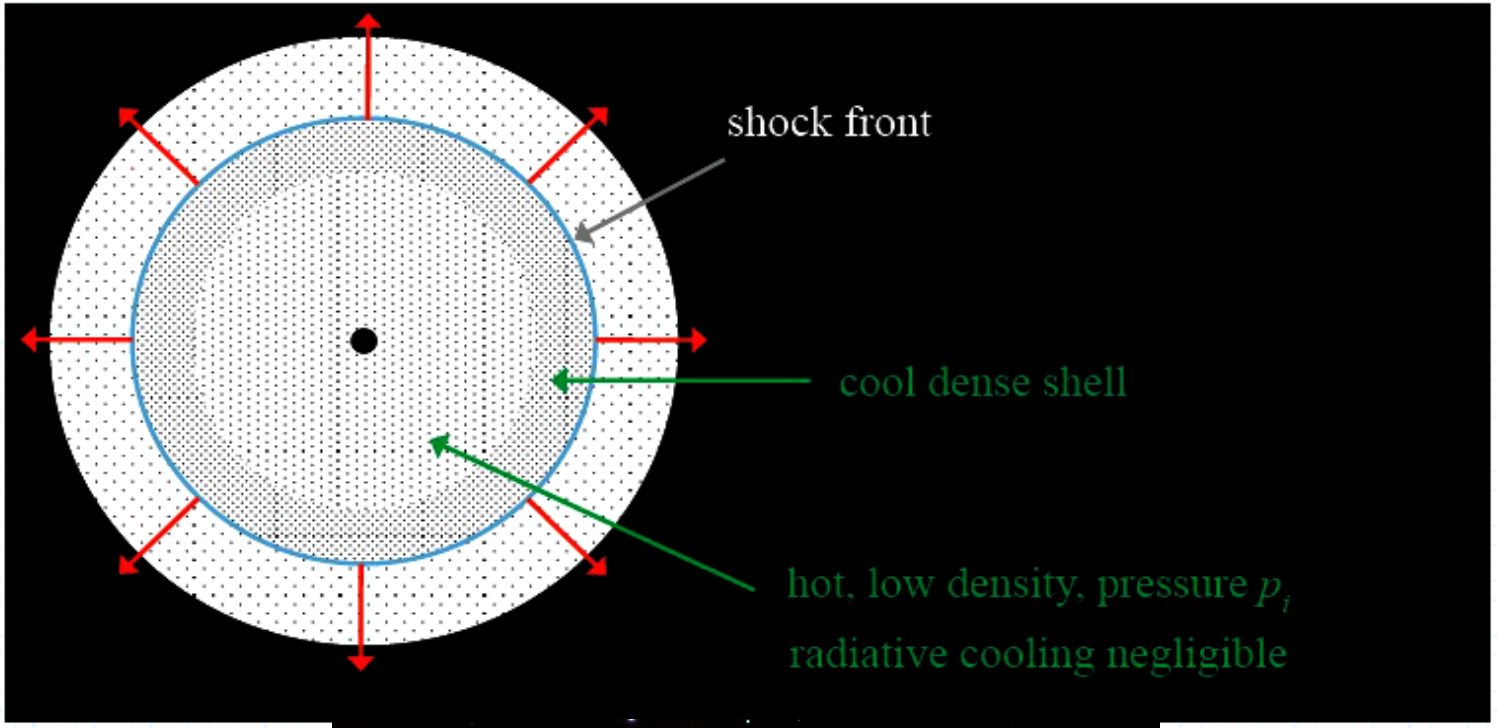
shock front
cool dense shell
hot, low density, pressure p_i
radiative cooling negligible

Summary phases of supernova shell expansion

1. Early phase ($m_{\rm swept} < m_{\rm ejecta}$):

   Free expansion, $R_{\rm s} = {\rm v}_{\rm s}\, t$

2. Sedov phase ($m_{\rm swept} > m_{\rm ejecta}$ and $t < t_{\rm rad}$):

   Energy conservation, $R \propto t^{2/5}$

3. Radiative "snowplow" phase ($t > t_{\rm rad}$):

   Momentum conservation, $R \propto t^{1/4}$ or $R \propto t^{2/7}$

4. Merging phase:

The kinetic energy of the shell is now transferred to the ISM. Detailed calculations show that the kinetic energy at fading is ~0.01 of the initial explosion energy

In this scenario $\varepsilon_{\rm SN} \sim 0.01$; almost all SN energy is radiated away...

Towards Higher Efficiency: Overlapping SNRs

In order to make SN feedback more efficient, one needs to ensure that another SN goes off inside the SNR before it has radiated away most of its energy.

This requires a SN rate $\zeta\,\dot{\rho}_* \geq \dfrac{3}{4\pi R_{\rm SN}^3\, t_{\rm SN}}$

If we set R_{SN} and t_{SN} to be the shock radius and time at the onset of the radiative phase, i.e., $t_{SN} = t_{rad}$ and $R_{SN} = r_{sh}(t_{rad})$, and we write $\dot{\Sigma}_* = \dot{\rho}_*/2H$ with H the scale-height of the disk, then we obtain

$$\dot{\Sigma}_* > 18.3\, M_\odot {\rm kpc}^{-2} {\rm yr}^{-1} \left(\frac{H}{0.2\,{\rm kpc}}\right) \left(\frac{\zeta}{10^{-2} M_\odot^{-1}}\right)^{-1} \left(\frac{n_{\rm H}}{{\rm cm}^{-3}}\right)^{1.82}$$

SuperNova Feedback (ejection)

To get a feel for whether the energy input from SN can be relevant for galaxy formation, imagine ejecting a mass $M_{\rm ej}$ from the center of a NFW dark matter halo.

This requires an energy injection of $E_{\rm ej} = \frac{1}{2} M_{\rm ej} V_{\rm esc}^2$. Using that, to a good approximation, the escape velocity from the center of a NFW halo is $V_{\rm esc} \simeq \sqrt{6\,c}\,V_{\rm vir}$ where c is the halo concentration parameter, we have that $E_{\rm ej} \simeq 3\,c\,M_{\rm ej}\,V_{\rm vir}^2$

The energy available from SN is $E_{\rm fb} = \varepsilon_{\rm SN}\,\zeta\,M_*\,E_{\rm SN}$

$\varepsilon_{\rm SN} \leq 1$ = fraction of SN energy available for feedback (not just radiated away)

$\zeta \simeq 0.01\,M_\odot^{-1}$ = number of SN produced per Solar mass of stars formed (IMF dependent)

$E_{\rm SN} \simeq 10^{51}\,{\rm erg}$ = energy supplied per SN

Equating $E_{\rm fb}$ to $E_{\rm ej}$ we obtain that $\dfrac{M_{\rm ej}}{M_*} \simeq 0.4\,\varepsilon_{\rm SN}\left(\dfrac{c}{10}\right)^{-1}\left(\dfrac{V_{\rm vir}}{200\,{\rm km/s}}\right)^{-2}$

Hence, even if 100% of the SN energy can be converted into kinetic energy of a galactic wind, SN can only eject about 40% of the stellar mass from a MW-sized halo.

This efficiency increases with decreasing halo mass; for $V_{\rm vir} = 50\,{\rm km/s}$ we have that $M_{\rm ej} \leq 6.4\,M_*$.

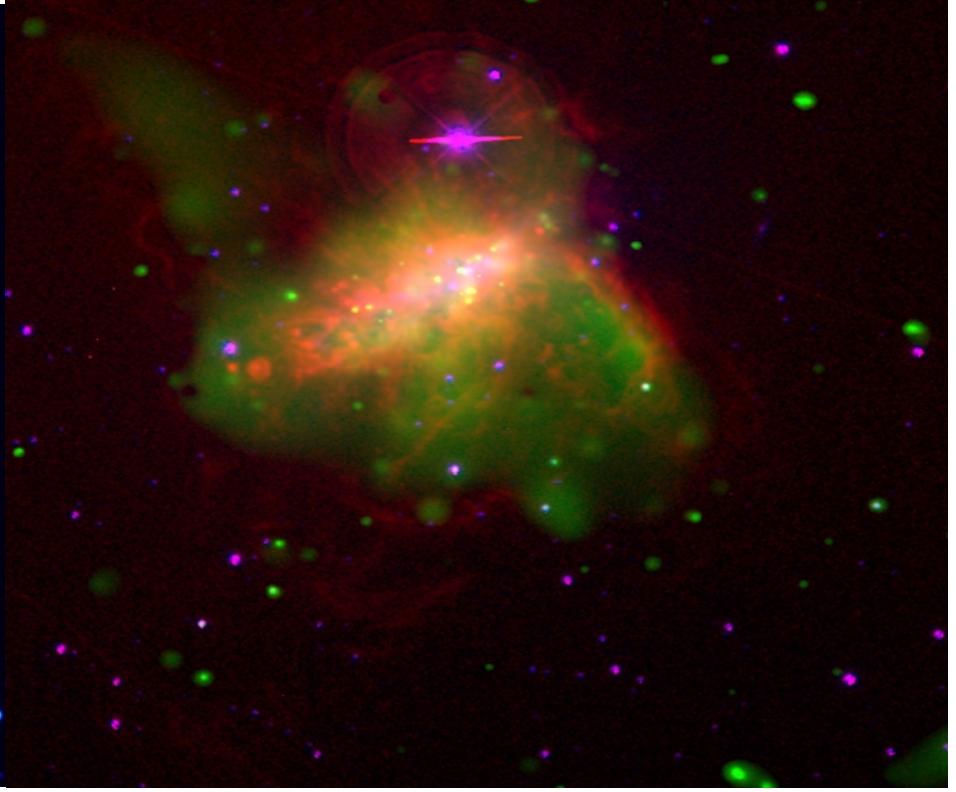

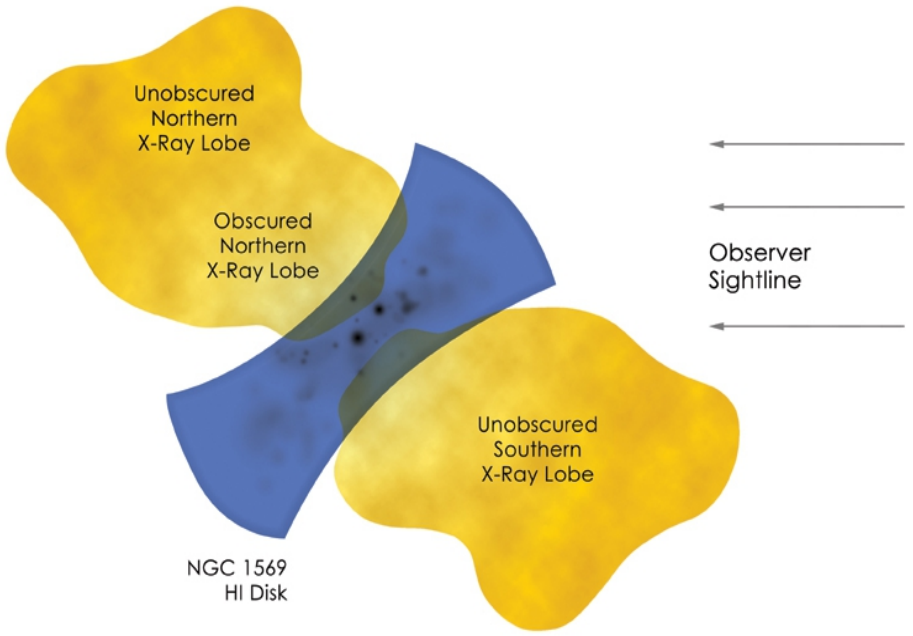

Direct observational evidence that these galactic winds drive metals out of the galaxy.

Through X-ray Spectroscopy: tight contraints on relative abundances of elements produced in Type II supernova explosions.

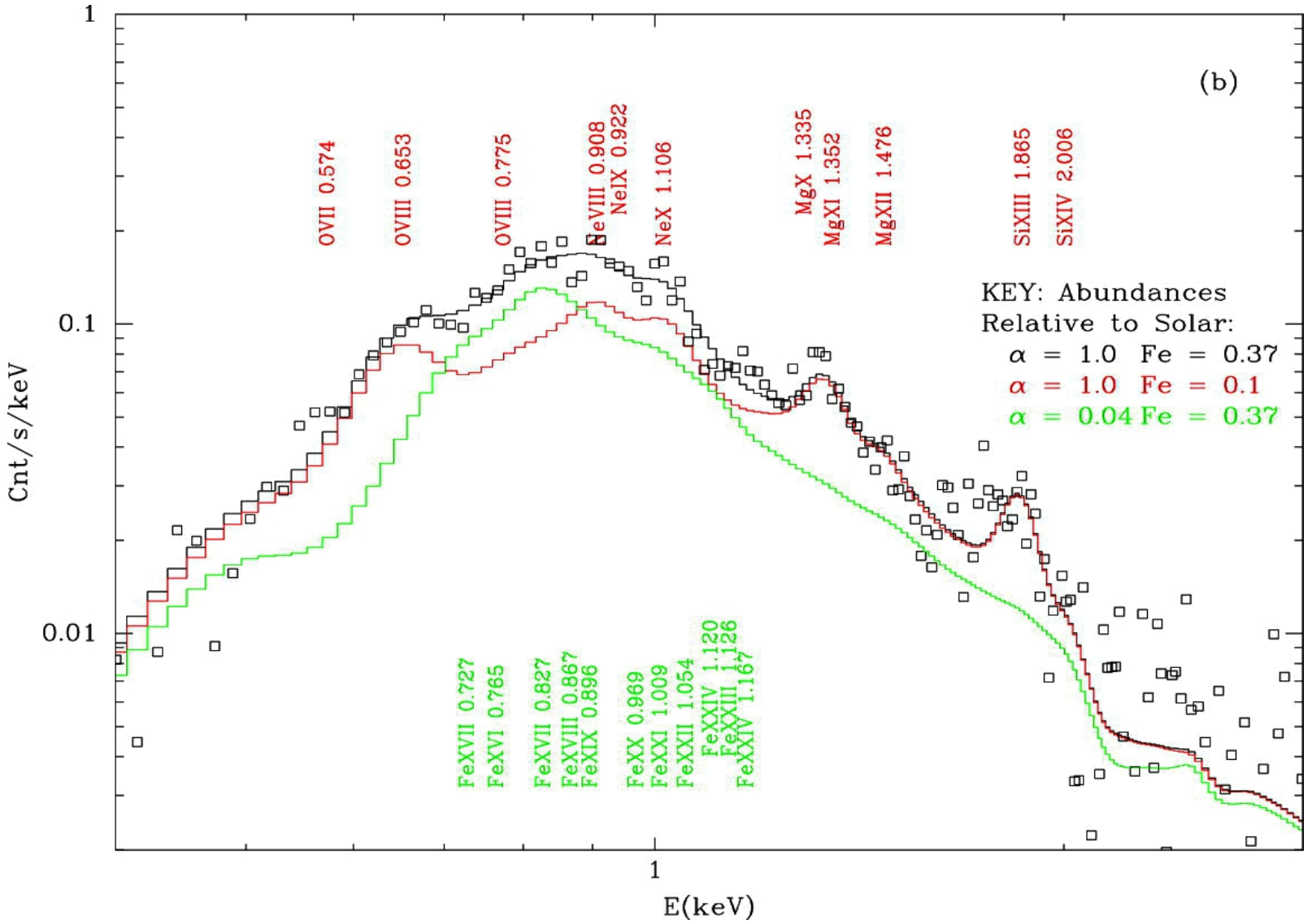

Temperature of hot gas around starburst galaxies constant as a function of the mass/rotation speed of the galaxy: this means gas is too hot to be in virial equilibrium with the dark matter halo of the smaller systems ==> escape

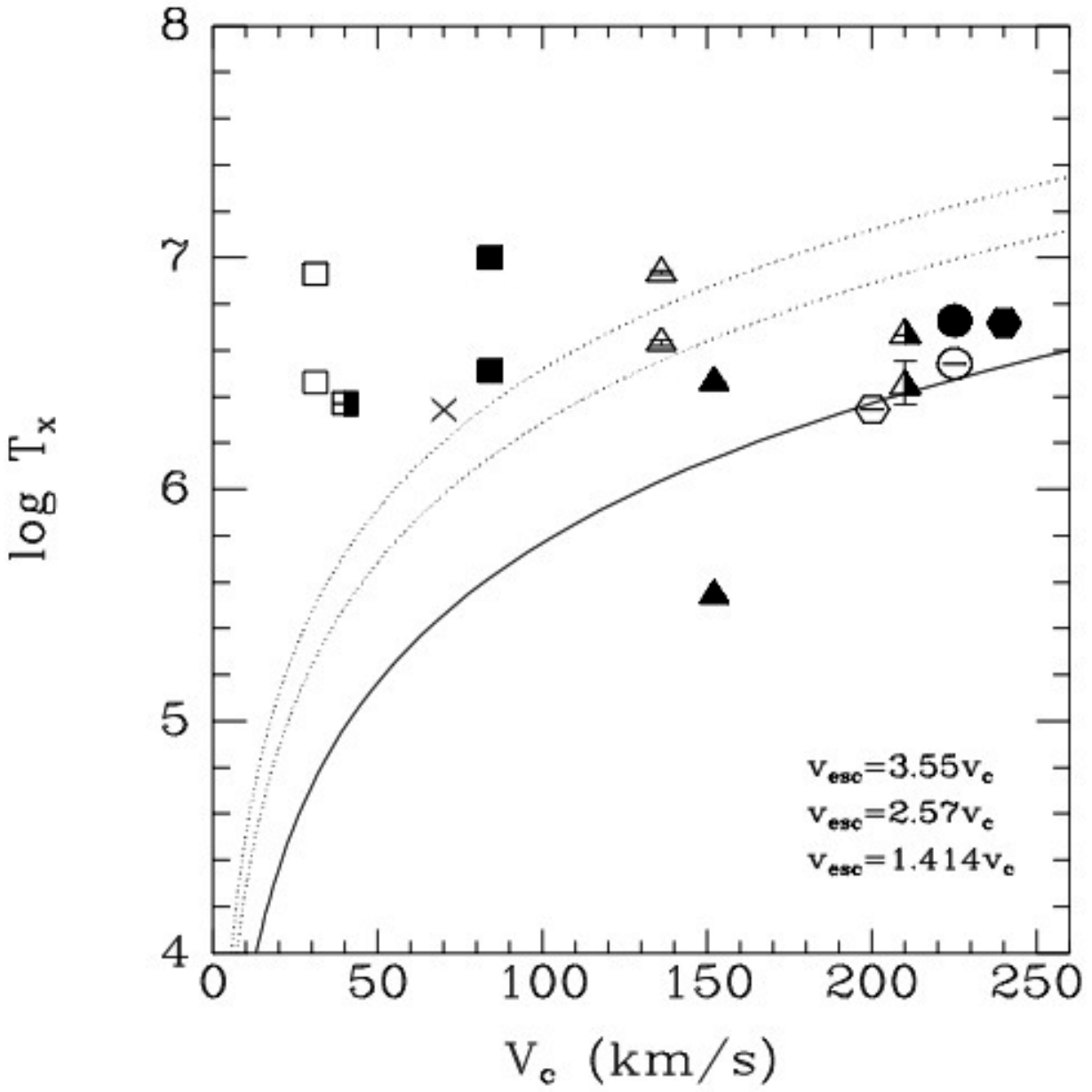

GALAXY MERGERS AND INTERACTIONS

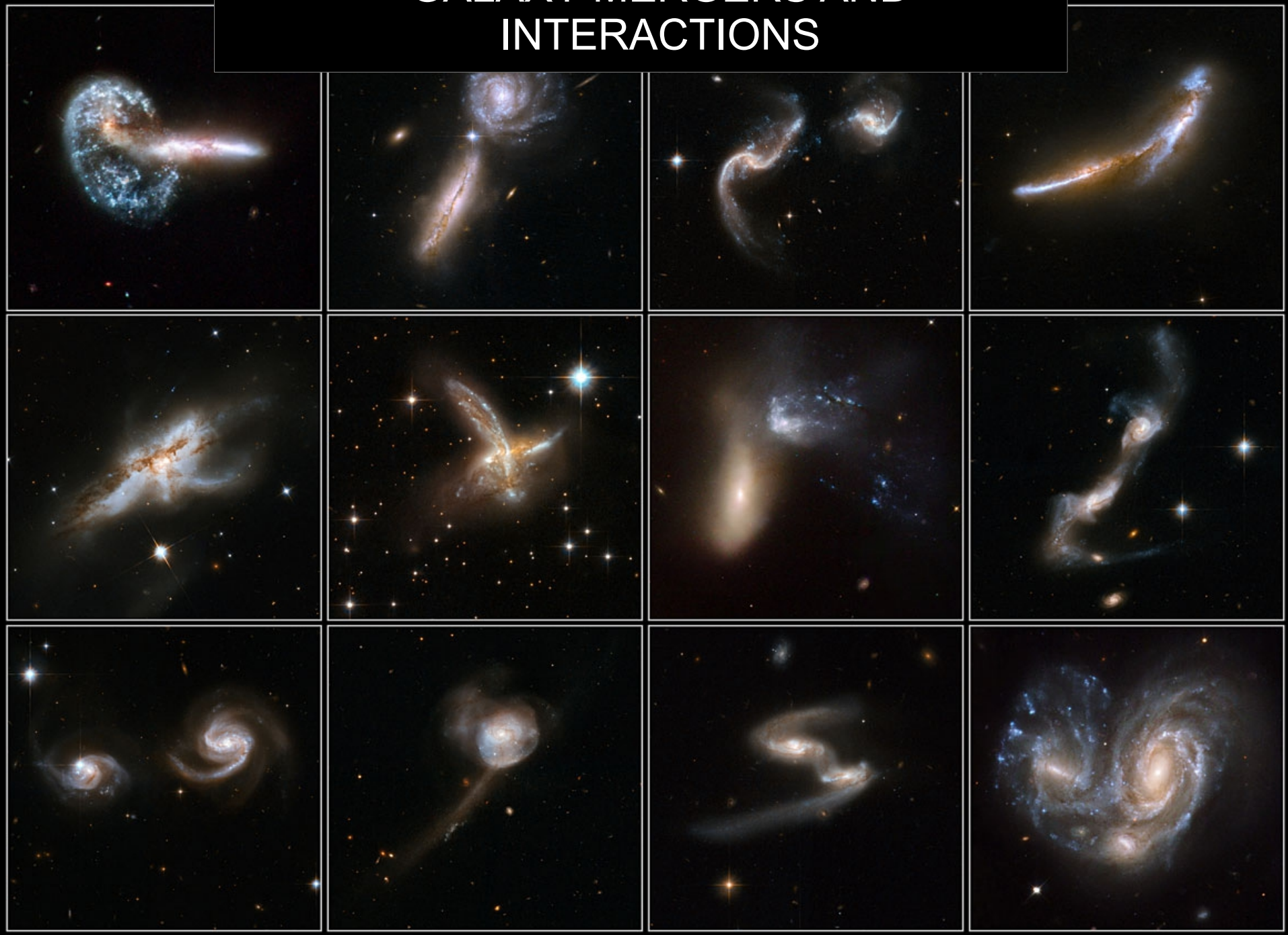

THE ASTROPHYSICAL JOURNAL, 178:623–666, 1972 December 15

GALACTIC BRIDGES AND TAILS

ALAR TOOMRE
Department of Mathematics, Massachusetts Institute of Technology
AND
JURI TOOMRE*
Department of Mathematics, New York University, and
Goddard Institute for Space Studies, New York
Received 1972 May 19

ABSTRACT

This paper argues that the bridges and tails seen in some multiple galaxies are just tidal relics of close encounters. These consequences of the brief but violent tidal forces are here studied in a deliberately simple-minded fashion: Each encounter is considered to involve only two galaxies and to be roughly parabolic; each galaxy is idealized as just a disk of noninteracting test particles which initially orbit a central mass point.

As shown here, the two-sided distortions provoked by gravity alone in such circumstances can indeed evolve kinematically into some remarkably narrow and elongated features: (i) After a relatively direct passage of a *small* companion, the outer portions of the primary disk often deform both into a near-side spiral arm or "bridge" extending toward this satellite, and into a far-side "counterarm." (ii) A similar encounter with an *equal* or more massive partner results typically in a long and curving "tail" of escaping debris from the far side of the victim disk, and in an avalanche of near-side particles, most of which are captured by the satellite.

Besides extensive pictorial surveys of such tidal damage, this paper offers reconstructions of the orbits and *outer* shapes of four specific interacting pairs: Arp 295, M51 + NGC 5195, NGC 4676, and NGC 4038/9. Those models can be found in the fairly self-explanatory figures 19, 21, 22, and 23.

Our present demonstrations will actually share the foremost of those flaws with Pfleiderer and Siedentopf: Like their examples, ours will be based exclusively on restricted three-body computations performed with massless particles which we pretend constitute the outer disks of pairwise interacting galaxies. By supposing these elements of either disk to move simply under inverse-square forces from the two mass points representing the bulk of each galaxy, we too will ignore all explicit self-gravity of the disk material (except in certain final estimates). Obviously this is an important sin of omission, and it is one which ought soon to be remedied, perhaps via some proper N-body calculations.

Retrograde encounters produce only small perturbations

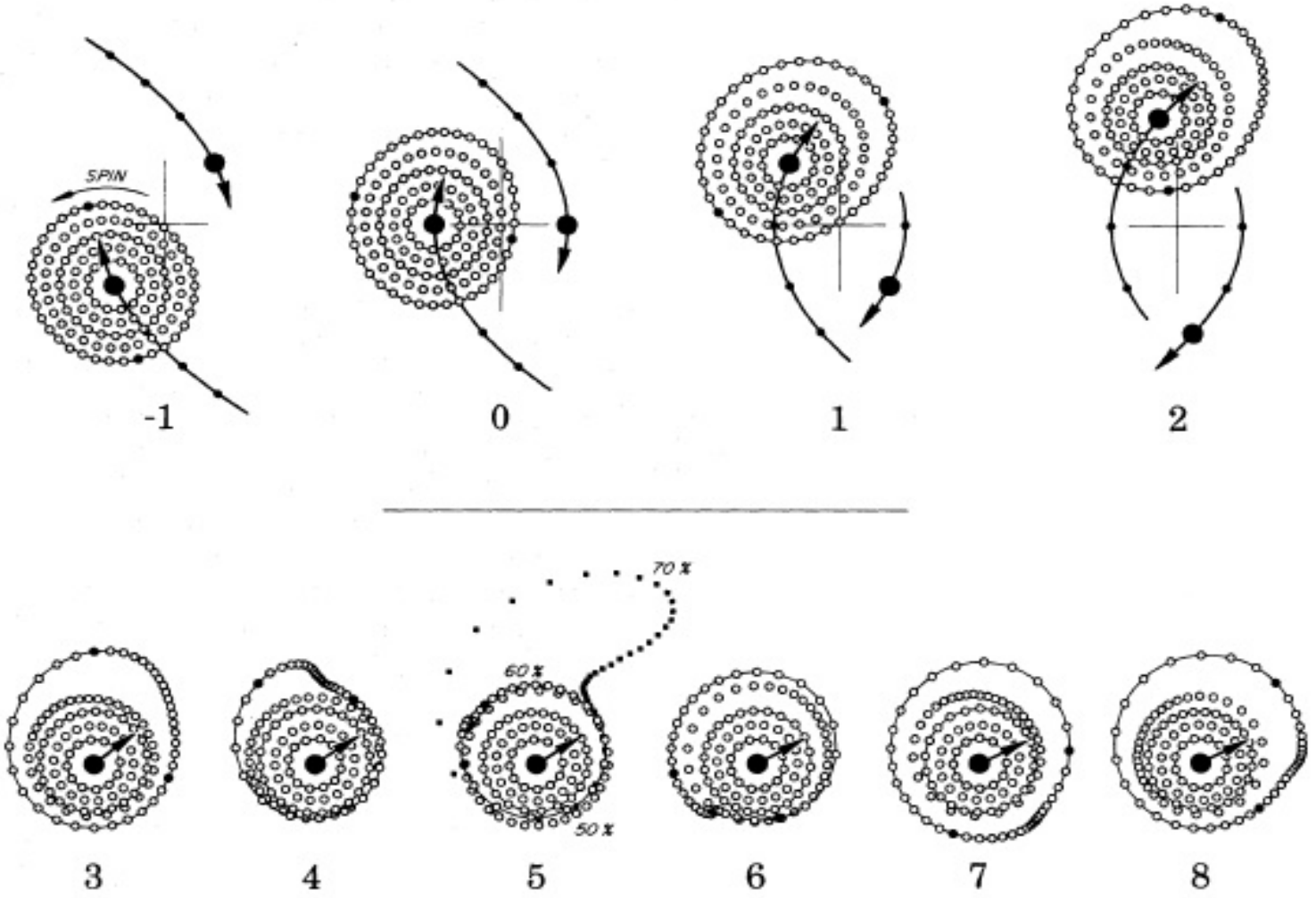

FIG. 1.—A flat retrograde ($i = 180°$) parabolic passage of a companion of equal mass. The two small filled circles denote test particles from the $0.6R_{min}$ ring which, in the absence of the encounter, would have reached positions exactly to the right and left of the victim mass at $t = 0$. The filled squares at $t = 5$ depict additional test particles from $0.7R_{min}$. (Note the partial interpenetrations of the outermost rings at $t = 4$, 5, and 6, and their continuing oscillations thereafter.)

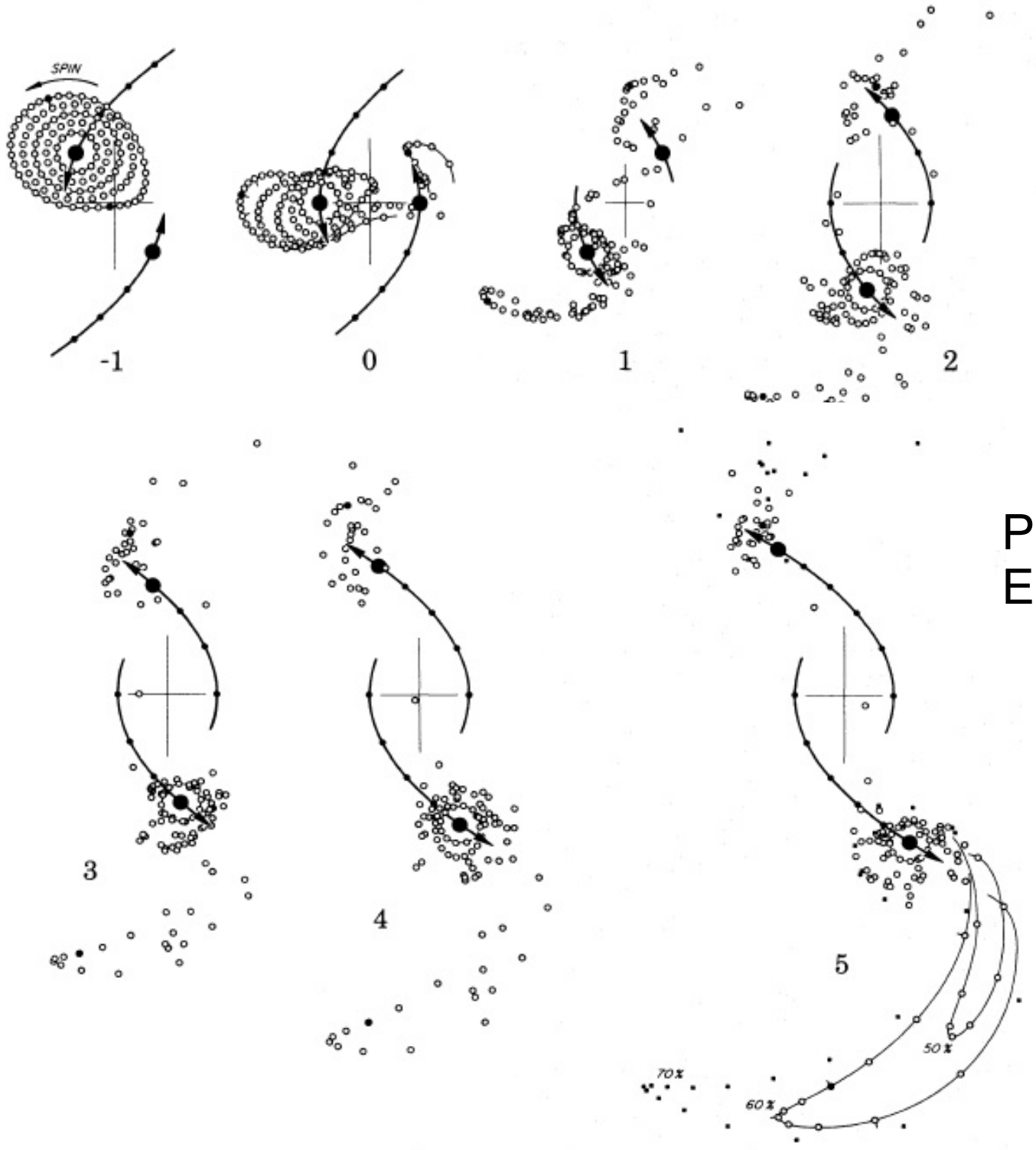

PROGRADE
ENCOUNTERS

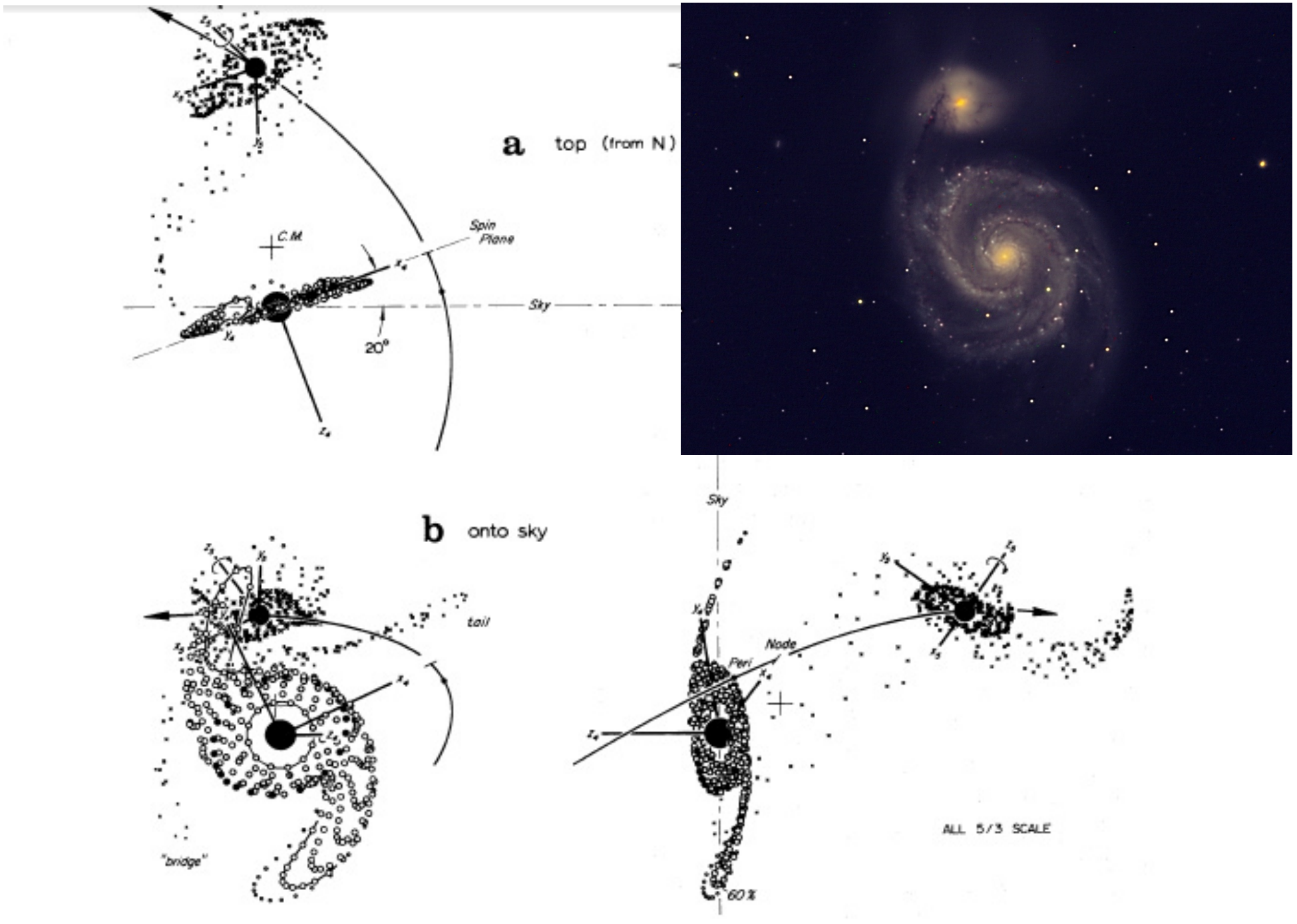

FIG. 21.—Model of the recent encounter between M51 and NGC 5195. Shown here at $t = 2.4$ are three mutually orthogonal views of the consequences of a highly elliptic $e = 0.8$ passage of a supposedly disklike "5195." This satellite was chosen to be one-third as massive, and of exactly 0.7 times the linear dimensions, of the "5194" primary—which itself contains particles from initial

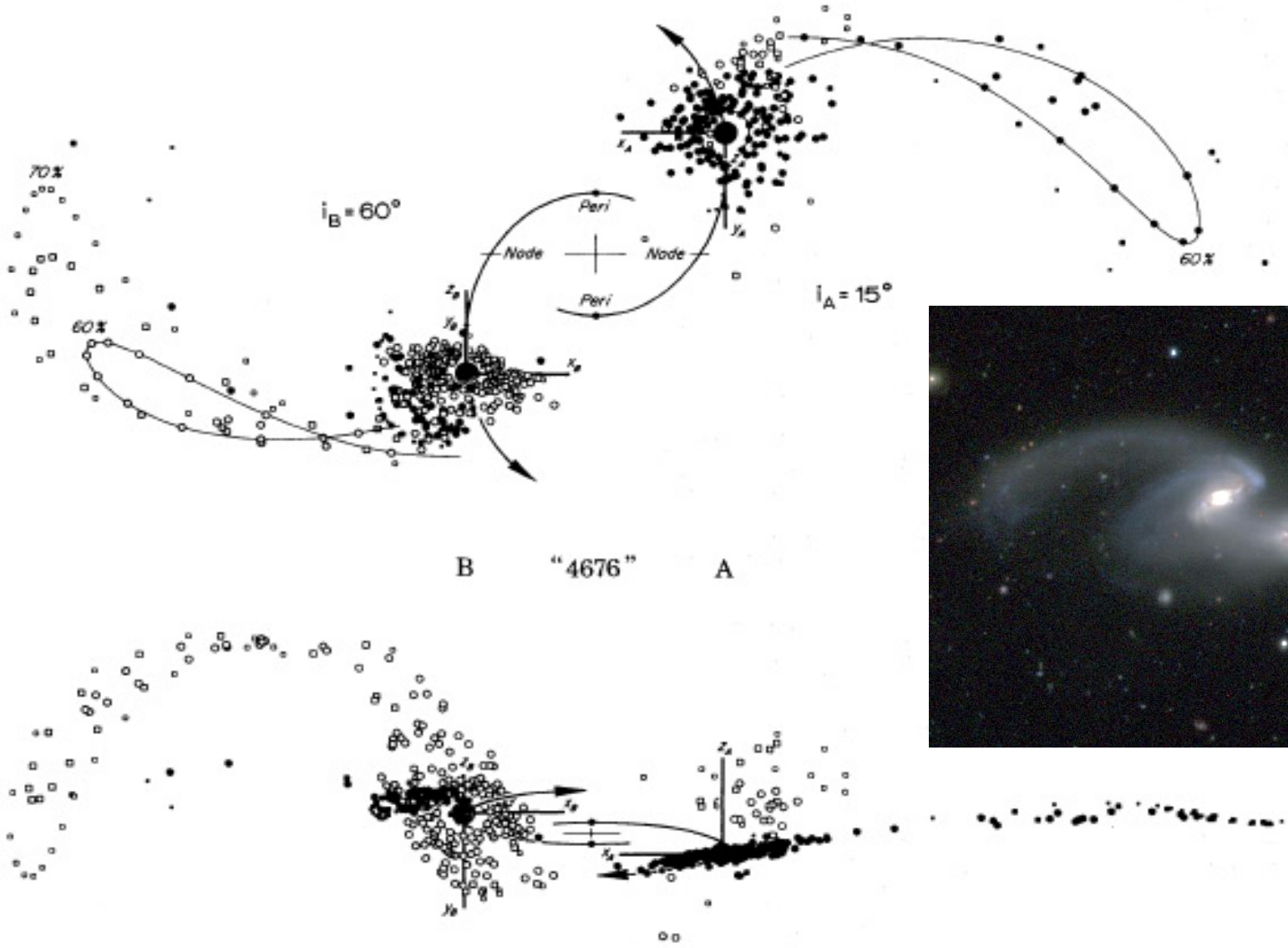

FIG. 22.—Model of NGC 4676. In this reconstruction, two equal disks of radius $0.7R_{\min}$ experienced an $e = 0.6$ elliptic encounter, having begun flat and circular at the time $t = -16.4$ of the last apocenter. As viewed from either disk, the adopted node-to-peri angles $\omega_A = \omega_B = -90°$ were identical, but the inclinations differed considerably: $i_A = 15°$, $i_B = 60°$. The resulting composite object at $t = 6.086$ (cf. fig. 18) is shown projected onto the orbit plane in the upper diagram. It is viewed nearly edge-on to the same—from $\lambda_A = 180°$, $\beta_A = 85°$ or $\lambda_B = 0°$, $\beta_B = 160°$—in the lower diagram meant to simulate our actual view of that pair of galaxies. The filled and open symbols distinguish particles originally from disks A and B, respectively.

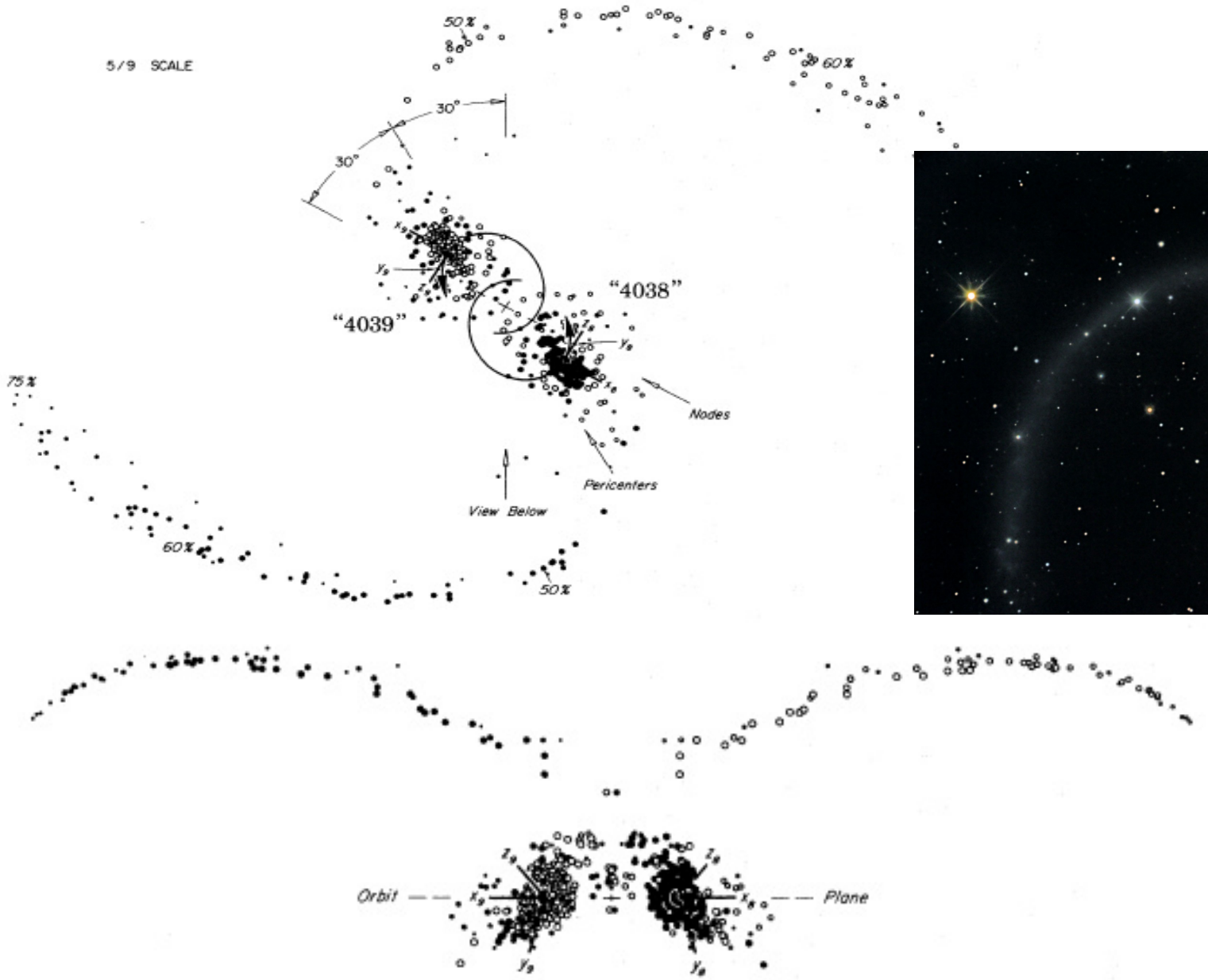

FIG. 23.—Symmetric model of NGC 4038/9. Here two identical disks of radius $0.75R_{\min}$ suffered an $e \approx 0.5$ encounter with orbit angles $i_8 = i_9 = 60°$ and $\omega_8 = \omega_9 = -30°$ that appeared the same to both. The above all-inclusive views of the debris and remnants of these disks have been drawn exactly normal and edge-on to the orbit plane; the latter viewing direction is itself 30° from the line connecting the two pericenters. The viewing time is $t = 15$, or slightly past apocenter. The filled and open symbols again disclose the original loyalties of the various test particles.

c) *Stoking the Furnace?*

We have deliberately not touched earlier on the well-known tendency (e.g., Burbidge *et al.* 1963; Zwicky 1967; Arp 1969*b*, 1971*b*; Stockton 1972) of the various tails, plumes, and intergalactic bridges to involve at least one galaxy whose own color or spectrum is often unusual, or which has a high surface brightness, or which contains oddly placed absorbing material and/or emitting regions.

That such intrinsic evidence of "strangeness" has itself contributed to the reluctance to regard the external features as tidal is both clear and understandable. Nevertheless —well short of such really exotic cases as the "jets" of M87 and 3C 273—we cannot help feeling that even this share of reluctance has been somewhat excessive: Would not the violent mechanical agitation of a close tidal encounter—let alone an actual merger—already tend to bring *deep* into a galaxy a fairly *sudden* supply of fresh fuel in the form of interstellar material, either from its own outlying disk or by accretion from its partner? And in a previously gas-poor system or nucleus, would not the relatively mundane process of prolific star formation thereupon mimic much of the "activity" that is observed?

TRANSFORMATIONS OF GALAXIES. II. GASDYNAMICS IN MERGING DISK GALAXIES

JOSHUA E. BARNES
Institute for Astronomy, University of Hawaii, 2680 Woodlawn Drive, Honolulu, HI; barnes@zeno.ifa.hawaii.edu
AND
LARS HERNQUIST[1]
Board of Studies in Astronomy and Astrophysics, U.C. Santa Cruz, Santa Cruz, CA 95064; lars@helios.ucsc.edu
Received 1995 February 27; accepted 1995 October 3

ABSTRACT

In mergers of disk galaxies, gas plays a role quite out of proportion to its relatively modest contribution to the total mass. To study this behavior, we have included gasdynamics in self-consistent simulations of collisions between equal-mass disk galaxies. The large-scale dynamics of bridge- and tail-making, orbit decay, and merging are not much altered by the inclusion of a gaseous component. However, tidal forces during encounters cause otherwise stable disks to develop bars, and the gas in such barred disks, subjected to strong gravitational torques, flows toward the central regions where it may fuel the kiloparsec-scale starbursts seen in some interacting disk systems. Similar torques on the gas during the final stages of a collision yield massive gas concentrations in the cores of merger remnants, which may be plausibly identified with the molecular complexes seen in objects such as NGC 520 and Arp 220. This result appears insensitive to the detailed microphysics of the gas, provided that radiative cooling is permitted. The inflowing gas can dramatically alter the *stellar* morphology of a merger remnant, apparently by deepening the potential well and thereby changing the boundaries between the major orbital families.

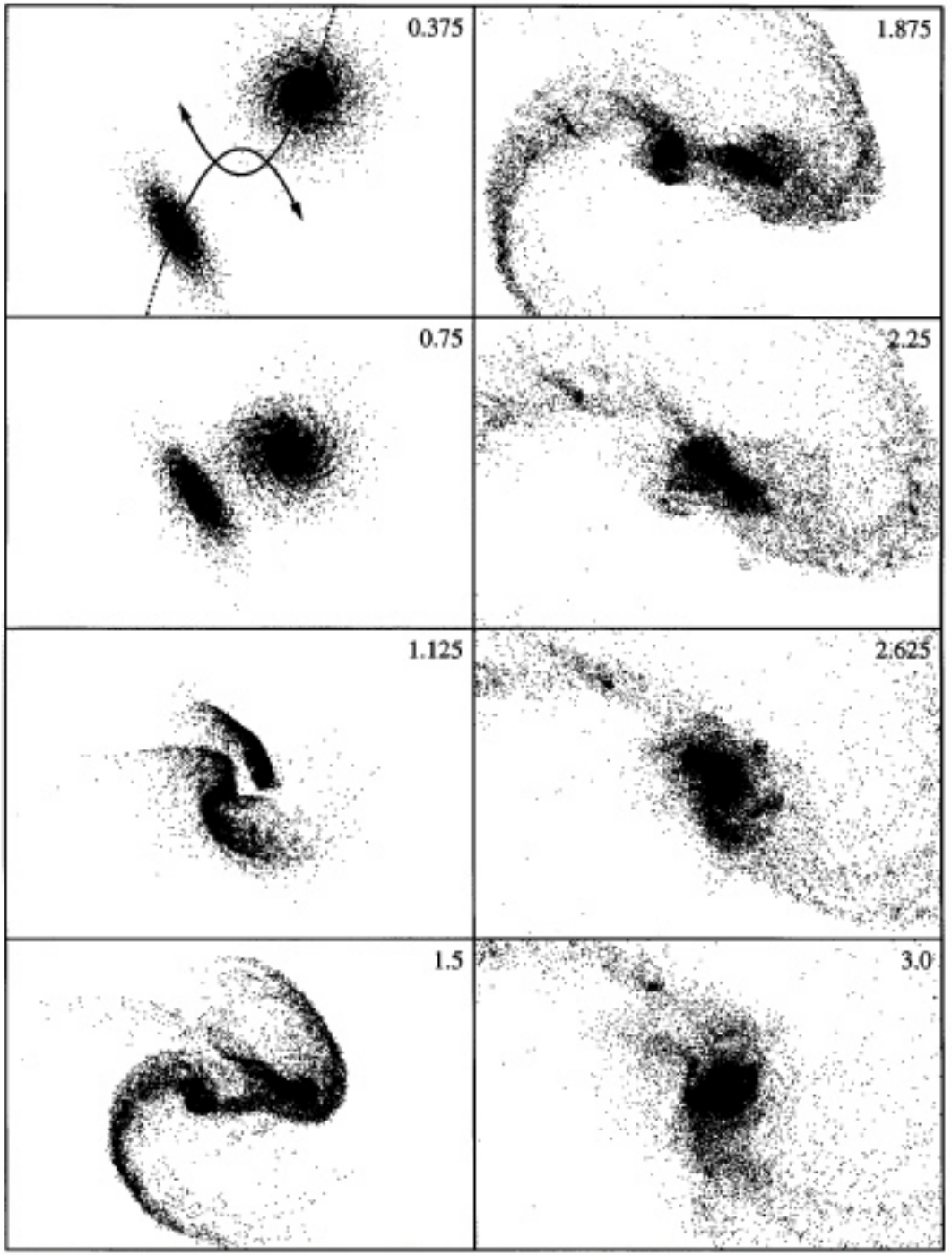

FIG. 4.—Evolution of the stellar distribution in encounter A, projected onto the orbital plane. The scale is the same as in Fig. 3.

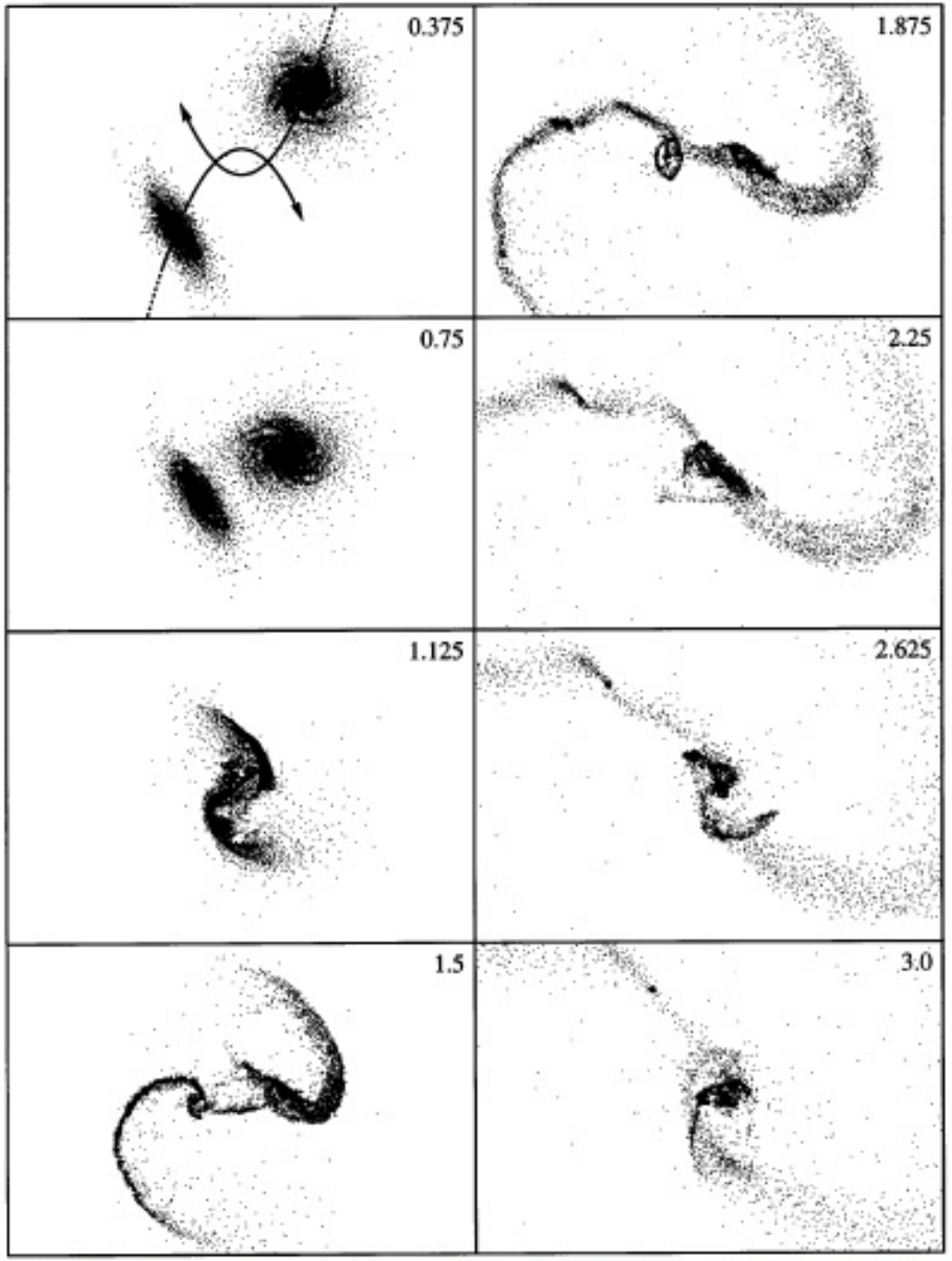

FIG. 3.—Evolution of the gas distribution in encounter A, projected onto the orbital plane. These frames are 3.6 × 2.4 length units; elapsed time is shown at the upper right of each. The first frame also shows the projected parabolic orbits of the infalling galaxies.

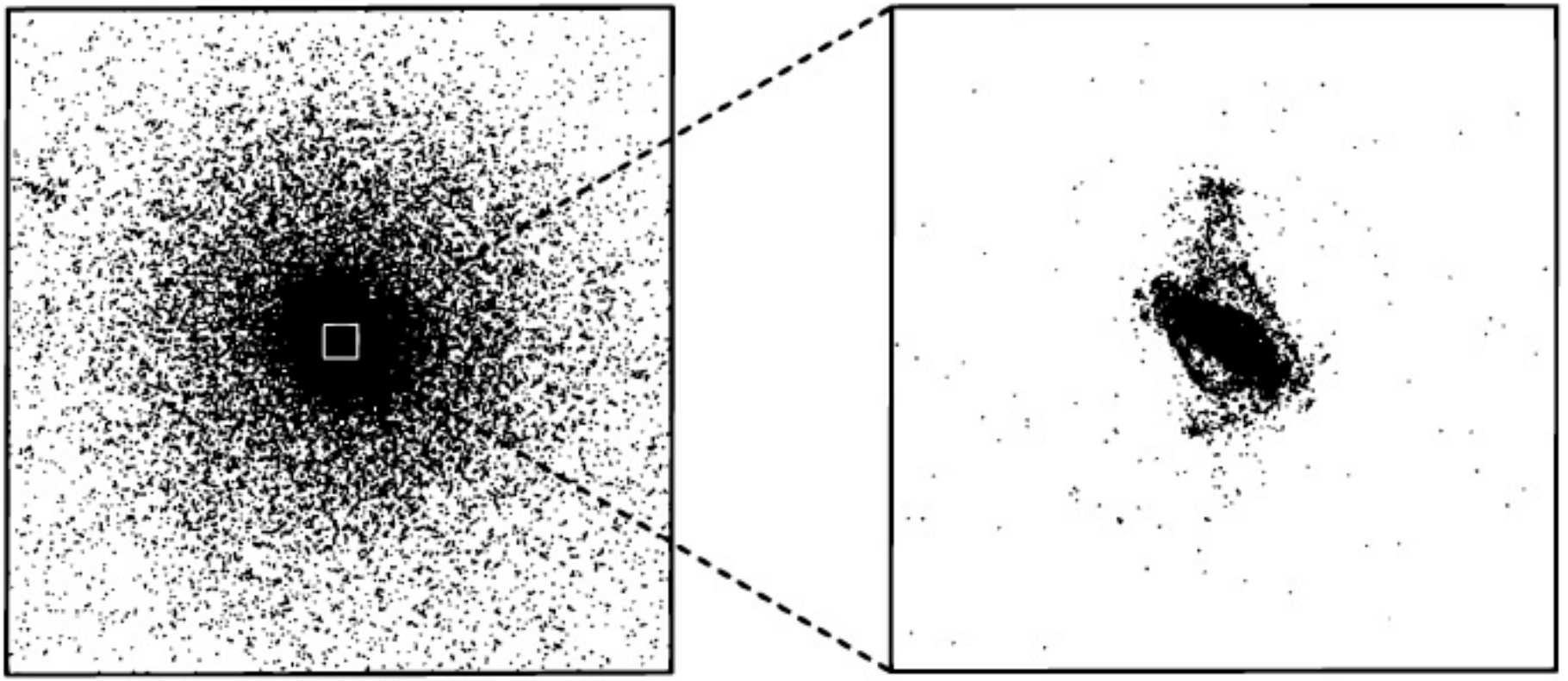

Do major mergers make elliptical galaxies?